LOCKHEED MARTIN ENERGY RESEARCH LIBRARIES
3 4456 0514400 0

CENTRAL RESEARCH LIBRARY
DOCUMENT COLLECTION

OAK RIDGE NATIONAL LABORATORY
operated by
UNION CARBIDE CORPORATION
NUCLEAR DIVISION
for the
U.S. ATOMIC ENERGY COMMISSION

ORNL-TM-3356

cy. 1

OFF-RESONANCE EFFECTS ON ELECTRONS IN MIRROR-CONTAINED PLASMAS

R. A. Dandl, H. O. Eason, P. H. Edmonds
and A. C. England

Thermonuclear Division

OAK RIDGE NATIONAL LABORATORY
CENTRAL RESEARCH LIBRARY
DOCUMENT COLLECTION
LIBRARY LOAN COPY
DO NOT TRANSFER TO ANOTHER PERSON
If you wish someone else to see this document, send in name with document and the library will arrange a loan.
UCN-7969
(3 3-67)

[This paper is being submitted for publication in Nuclear Fusion.]

NOTICE This document contains information of a preliminary nature and was prepared primarily for internal use at the Oak Ridge National Laboratory. It is subject to revision or correction and therefore does not represent a final report.

This report was prepared as an account of work sponsored by the United States Government. Neither the United States nor the United States Atomic Energy Commission, nor any of their employees, nor any of their contractors, subcontractors, or their employees, makes any warranty, express or implied, or assumes any legal liability or responsibility for the accuracy, completeness or usefulness of any information, apparatus, product or process disclosed, or represents that its use would not infringe privately owned rights.

ORNL-TM-3356

Contract No. W-7405-eng-26

OFF-RESONANCE EFFECTS ON ELECTRONS IN MIRROR-CONTAINED PLASMAS

R. A. Dandl, H. O. Eason, P. H. Edmonds,
and A. C. England

THERMONUCLEAR DIVISION

APRIL 1971

[This paper is being submitted for publication in Nuclear Fusion.]

OAK RIDGE NATIONAL LABORATORY
Oak Ridge, Tennessee
operated by
UNION CARBIDE CORPORATION
for the
U.S. ATOMIC ENERGY COMMISSION

LOCKHEED MARTIN ENERGY RESEARCH LIBRARIES

3 4456 0514400 0

OFF-RESONANCE EFFECTS ON ELECTRONS IN MIRROR-CONTAINED PLASMAS*

R. A. Dandl, H. O. Eason, P. H. Edmonds,
and A. C. England

Oak Ridge National Laboratory
Oak Ridge, Tennessee 37830

ABSTRACT

Resonant heating by microwave power has been used to produce high-β plasmas with electron temperatures near 1 MeV. Typically plasmas are produced with $\omega_{pe} \sim \omega_{ce}$. Further experimental heating studies described here have shown that a large increase in stored plasma energy is produced by microwave power with a frequency higher than the cold-electron resonance frequency. This increase, caused by off-resonance heating, is attributed both to stochastic heating and to the control of an instability through changes in the electron distribution function. Alternatively, a decrease in the stored plasma energy is produced by microwave power at a frequency below the cold-electron resonance frequency. This effect is attributed in part to enhanced diffusion into the loss cone. However, a small fraction of the plasma is heated to high energies.

---

*Research sponsored by the U. S. Atomic Energy Commission under contract with the Union Carbide Corporation.

1. INTRODUCTION

Energetic electron plasmas have been produced by a resonant microwave heating source in a simple magnetic mirror geometry [1-4]. In these early experiments the resonant power was supplying off-resonant heating through Doppler frequency shifts, relativistic resonance charges, etc., as evidenced by the high-electron energies achieved. Clearly these energies could not be explained by simple resonance. However, in these early experiments, a separation of the resonant and off-resonant effects could not be made because a single-frequency microwave power source was used.

For optimum energy storage, it was empirically established that the mirror ratio for the resonance modulus-B surface should lie approximately halfway between the midplane and the mirror maximum. For example, with a 2:1 Mirror Ratio, R, the mirror ratio at Resonance, $R_\mu \simeq 1.4$ to 1.6. For values of $R_\mu \lesssim 1.2$, the plasmas were unstable and contained little stored energy.

These poor results were attributed in part to the highly anisotropic heating for electrons near the midplane. The high anisotropy could be responsible for various instabilities.

Recently, we have reported [5-7] effective off-resonant heating by microwave power at a frequency above the cold-electron resonant frequency. These studies are described in Sec. 2 under the heading of "Upper Off-Resonant (UOR) Heating."

We have also reported [7] on driven losses with microwave power at frequencies below gyroresonance. These studies are described in Sec. 3 under the heading of "Lower Off-Resonance (LOR) Heating."

In a recent theory, Grawe [8] has calculated the heating rate of electrons by microwaves in simple magnetic mirrors. He finds the heating rate for relativistic electrons which do not cross resonant modulus-B contours (on which the microwave frequency equals the non-relativistic cyclotron frequency) can be comparable to low-energy electron heating rates. These heating rates are a strong function of the mirror ratio for the resonant modulus-B contour. The results of a series of calculations based on Grawe's theory are displayed in Fig. 1. The important points to be noted are as follows: (1) The heating rate for low-energy electrons increases rapidly as the resonant mirror rate decreases (or as the axial magnetic gradient decreases). As mentioned before, this would give rise to high anisotropy. Because of the large source of low-energy electrons from ionization, these heating rates would be responsible for the maintenance of the warm non-relativistic plasma. (2) The heating rate for relativistic electrons is relatively independent of the resonant mirror ratio (or the axial magnetic gradient). This is due to the non-resonant nature of the heating. Still the heating rate can be higher than that for low-energy electrons. Naturally, the very high-energy particles are also subject to other energy loss mechanisms (like synchrotron radiation) which are not considered here but which play an important role in the equilibrium.

Heating rates have not been measured in the experiments reported here. Hence, we have no specific comparisons with Grawe's theory. Nevertheless, some corroborative evidence is presented below that suggests qualitative agreement with this model. This and other theoretical comparisons will be discussed in Sec. 2, D.

It has been suggested that Grawe's treatment contains mathematical approximations such that the heating rate under some conditions (e.g., at low-electron energies) is underestimated. Although detailed comparisons with heating rates (cf. Fig. 1) are not justified, the basic physical model used by Grawe is not in question, and much of the calculation qualitatively agrees with experiment.

The investigations reported here have all been carried out in the ELMO apparatus which is shown in Fig. 2. It consists of a perforated copper cavity situated in a vacuum chamber and surrounded by two pairs of magnetic field coils which allow operation with a variable mirror ratio. The apparatus has been described in detail elsewhere [3-5].

A set of waveguides is installed in ELMO to allow simultaneous application of power at two or three frequencies. Sources that have been used are: (1) a 10.6-GHz, 3-kW continuous-wave klystron power source; (2) a 35.7-GHz power source consisting of one or two traveling-wave-tube (TWT) oscillators each able to supply up to ~900 W of power; (3) a 55-GHz, ~5-kW continuous-wave power source. All of these power sources have not always been simultaneously present during the entire course of this experimental program.

2. UPPER OFF-RESONANT HEATING

A. HIGH-β PLASMA PRODUCTION

In the experiments to be described in this section, the magnetic field is adjusted either: (1) to allow resonance for the 10.6-GHz (3 cm) source with the 35.7-GHz (8.4 mm) or the 55-GHz (5.5 mm) sources supplying the upper off-resonant power; or (2) to allow resonance for the 35.7-GHz source with the 55-GHz source supplying the upper off-resonance.

Figure 3 demonstrates the effect of the upper off-resonant (UOR) heating on the stored energy and temperature. In this experiment, the resonant power level was held constant at 880 W and the off-resonant power varied. The resonant power produced a plasma with a $\beta \simeq 5\%$. The stored energy calculated from diamagnetic effects increased by about a factor of 6 when the UOR power level reached the resonant power level. At the highest UOR power level, the amount of stored energy, measured diamagnetically, reached ~150 J, which corresponds to a $\beta \gtrsim 75\%$ for an assumed 1-liter plasma volume. The change in the electron temperature, T_e, is small (perhaps 50%) as measured from the bremsstrahlung radiation. The electron density, n_e, also measured from the bremsstrahlung radiation shows a marked increase, indicating that it is the quantity that has increased.

The neutron rate increases by more than an order of magnitude with full off-resonant power. The neutrons are believed to be due to the Coulomb dissociation of deuterium, the feed gas, by those electrons whose energies exceed the binding energy of the deuteron, 2.22 MeV.

This same effect can be seen with 10.6-GHz resonant power and either 35.7-GHz or 55-GHz upper off-resonant power. Figure 4 shows the various plasma parameters as a function of 35.7-GHz UOR power. The diamagnetically measured stored energy, $W_\perp$, increases by more than an order of magnitude as the 35.7-GHz power is increased. The increase results principally from increased density, n_e, since the temperature, T_e, has increased by only ~50%. In this case the neutron rate is quite small because of the much lower hot-electron density as compared to the 55-GHz UOR heating. In spite of the saturation shown by the density and stored energy, the plasma β exceeds 50% in the high-power region.

B. ANNULAR PLASMA CHARACTERISTICS

1. Skimmer Probe Scans

As reported previously [4], the energetic component of the plasma resides in an annular region near the midplane. The first determination of this configuration was made with skimmer probes in a plasma supplied with only resonant power at 35.7 GHz. Probes could be inserted radially inward and radially outward to give rough indications of the plasma's mean radius and shell thickness; however, since the probes exerted such a major perturbation on the plasma, only qualitative estimates of the radius and shell thickness could be given.

Figure 5 shows the effect on the stored energy produced by the probe scans from both the outside inward and from the inside outward. The inside outward scan was made with an off-axis probe having a right angle bend at the end. The probe could be rotated so that the end went from the axis to a maximum radius of ~11 cm. Figure 6 shows the effects on the stored energy of a probe scan from the outside inward made on a plasma supplied with 3-cm resonance and 8-mm off-resonance heating. Although the details differ, the basic shape of the curve is quite similar to the inward-going probe curve of Fig. 5, indicating that the off-resonant heating also gives rise to an annular-shaped plasma.

2. Magnetic Field Measurements

Subsequently, the magnetic field produced by the plasma was measured by Hall probes both on-axis and off-axis outside the cavity. These measurements were analyzed and current distributions in the plasma region consistent with the measured fields could be calculated [9]. These current distributions indicated that the plasma volume was ~1 liter and that the mean radius was ~7 cm with a width of ~2 cm.

Figure 7 shows the surface current distribution calculated for a plasma produced by 2 kW of 35.7-GHz resonant power [9]. The current distribution produced a field depression in the plasma region consistent with a β of ~40%. The magnetic field modulus-B contours for this case are displayed in the upper half of Fig. 8. The region of high β is clearly evident. The lower half shows the modulus-B contours for the vacuum field. Under more favorable conditions than allowed under the restrictions of reproducible stable plasma formation required by the probe measurements, it was clear that much higher β could be obtained under the assumption of a constant plasma volume.

Even though the data shown here are for 35.7-GHz resonant power, clearly some of the power was being used to heat the high-energy particles off-resonantly.

3. Calorimetry

Evidence for the annular characteristic of the plasma has also been obtained from a scanning calorimeter placed in the mirror throat. The radial resolution of the calorimeter was very broad as the calorimeter had an effective diameter of 1.5 cm. Located in the throat, the calorimeter was sensitive primarily to the cold plasma produced by ionization and lost out the mirror. The power dissipated on the calorimeter results from the recombination of electrons and ions, thermal particle energy, and directed particle energy due to the space potential. Hence the resulting signal may not give a true indication of the location of the maximum region of ionization.

Other effects are also present. The plasma flow out the mirror at large radii is spread over a larger area and hence the calorimeter signal

must be multiplied by a correction factor (the area of the annulus intercepted by the probe divided by the probe area) which is roughly proportional to radius at large radii. The signal can be interpreted as due to plasma flowing along field lines from near the midplane, hence the radial location of the maximum calorimeter power production region can be found at the midplane by following the self-consistent field lines back to the midplane. At very large radii the throat of the cavity shields the outer portion of the calorimeter from plasma flow from the midplane, hence the signal will be attenuated.

Figure 9 shows the power dissipated on the calorimeter as a function of radius. On the bottom scale is the calorimeter radius in the mirror throat and on the top scale is the radius of a field line passing through the calorimeter and followed back to the midplane along a field line calculated for the self-consistent plasma plus vacuum magnetic field.

The lower dashed curve shows the amount of power dissipated on the calorimeter with 10.6-GHz resonant power only. The dot-dash curve shows the power dissipated on the calorimeter by the plasma when supplied with both 10.6-GHz resonance power and 35.7-GHz UOR power. The annulus is clearly visible as it is in the difference curve. The signal drop-off beyond a 6.5-cm radius (bottom scale) is due to the shadowing effect of the mirror throat.

Multiplying the curves by the factor accounting for the increased area at large radii moves the peak to a radius of ~6 cm (on the top scale), not inconsistent with the results obtained from the diamagnetic measurements. However, because of the above-mentioned factors, this should not be considered a measure of the annulus mean radius, but only as a corroborative data supporting our previous measurements.

The plasma flow out the end is not azimuthally symmetrical as evidenced by a variation in probe power when the probe is rotated both above and below the axis. This may be due to inhomogeneities in the magnetic field, or microwave power feed, etc. It prevents us from making an accurate power balance measurement.

Ikegami et al. [10] have also observed an annular plasma in a mirror machine. The annular characteristic is attributed to heating at the second harmonic. In the experiments reported in Ref. [10], the mirror ratio is ~3.3 so that the region of second-harmonic resonance (a magnetic field half the field for cold-electron resonance) is always present. In ELMO, the mirror ratio is lower and the field for second-harmonic resonance is generally outside the cavity, or, if present, at a larger radius than the radius of the hot-electron annulus.

C. INSTABILITY STUDIES

1. Instability Identification

The existence of a microscopic type of instability has long been recognized in our resonantly fed plasmas, in addition to the well-documented MHD type of macroscopic instability [11]. This microinstability is observed in the warm plasma produced by the resonant power and is manifested by the emission of radiation at a frequency very near one half of the applied resonant microwave frequency. This instability is observed on electrostatic probes when the mirror ratio at the cold-electron heating zone, R_{μ_o}, is below ~1.4. Such a low value of R_{μ_o} implies that the axial magnetic gradient is small and hence that the cold electrons acquire high anisotropy while being resonantly heated.

Figure 10 shows the output of a spectrum analyzer in a band around 5.32 GHz at low 10.64-GHz power. The radiation appears after the 10.64 GHz has crossed a power threshold of 160 W for this particular set of plasma parameters. It is within one part in 5×10^3 of the half frequency of the microwave power. However, as the power is raised, cavity modes may be excited by the instability and these other frequencies tend to confuse the interpretation as seen at the higher 10.64-GHz power levels. If the conditions for onset can be just barely met, then only the half frequency is observed.

At higher resonant power conditions, the instability (now occurring at discrete frequency bands near the half harmonic) appears as short bursts on the spectrum analyzer coincident with energetic electron losses into the mirror loss cone. The instability has also been observed with 35.7-GHz resonant heating; the instability again appearing near the half harmonic of the oscillator or approximately 17.85 GHz.

This instability has been tentatively identified as the electron analog of the electrostatic ion mode first described by Timofeev [12] and the subject of further current work [13]. This is an electrostatic velocity space instability driven by a temperature anisotropy requiring $T_\perp/T_\parallel \gtrsim 6$ for instability.

Theoretical arguments mentioned earlier suggest that off-resonant heating would tend to decrease anisotropy because of heating throughout the volume rather than on specific modulus-B surfaces as in resonant heating. Hence, a reasonable explanation for some of the effectiveness is in the suppression of the instability through UOR heating by lowering of the anisotropy. Other possible stabilizing factors are relativistic effects as may operate in Astron [14, 15].

Figure 11 shows the amount of UOR power required to suppress the instability as a function of the resonant 10.6-GHz power. The resonant power level determines the anisotropy and the cold- and warm-plasma densities. For the low gas pressure case of 1.8×10^{-5} Torr, the amount of UOR power appears to increase monotonically with the resonant power level. For the high-pressure case (2.0×10^{-5}), there is a saturation of the amount of UOR power required followed by a sharp increase.

Figure 12 shows the diamagnetically measured stored energy produced by just that UOR power required to stabilize. The stored energy is plotted as a function of resonant power showing that energy stored before and after UOR power is applied. The change is quite marked and is due both to the instability suppression as well as to the increased heating efficiency of the UOR power.

For power levels beyond those shown here, the plasma makes a transition into the "dark" mode, a mode characterized by low stored energy, high fluctuating electric fields and little excitation light. The plasma potential as measured by an electron beam is large and negative. The parameter variation at high-power levels, as shown in Figs. 11 and 12, is probably strongly influenced by the incipient changes in plasma potential and changes in cold-plasma density.

D. THEORETICAL COMPARISONS

A number of theoretical treatments of cyclotron heating have appeared in the literature in the past. Early attempts by Seidl [16] and Piliya and Frenkel [17] indicated effective heating involving stochastic processes for non-relativistic electrons. More recently the stochastic treatment of Grawe [8], mentioned earlier, with relativistic effects taken into account

shows effects in qualitative agreement with our results. Qualitative agreement is found in the measured high temperature as compared to theory, the fact that off-resonant heating rates are large, and the fact that the particles tend to be confined toward the midplane. Unfortunately, Grawe's chief results are expressed in terms of heating rates which are not easily measured experimentally. Other theories have recently appeared, such as those by Eldridge [18] and Sprott [19], but few definitive comparisons have been made. One measurement of the perpendicular diffusion coefficient, $D_\perp$, which we will describe later, is in agreement with Eldridge [18]. However, the lack of other theoretical comparisons is unfortunate — only Eldridge has a theoretical determination of this quantity for comparison.

Sprott's theory calculates the perpendicular and parallel heating rates in terms of an effective collision frequency. The theory gives a plausible, but yet unproven, explanation of the results discussed in Sec. 3 dealing with the driven losses with lower off-resonant power.

3. LOWER OFF-RESONANT DRIVEN LOSSES AND HEATING

A. EXPERIMENTAL ARRANGEMENT

As we have already described, off-resonant power at short wavelengths has been found to be very efficient in plasma heating. Based on this knowledge, the logical alternative was attempted; plasma heating at long wavelengths. The motivation for this is that low-frequency microwave power is relatively inexpensive and readily available. Also, the microwave technology at long wavelengths is much simpler than that for short wavelengths. A conveniently available 10.6-GHz source of nominally 5-kW continuous wave was used for the lower off-resonance heating and 35.7 GHz was used for the resonance heating--the resonant breakdown and production of a modest-β plasma.

As shown in Fig. 2, the 10.6-GHz power was added through an axial guide into the end of the cavity. The nominal cold-plasma density is high enough so that the plasma frequency might be greater than the microwave frequency. However, whistler mode propagation was believed to be possible when the plasma density was high enough so that the ordinary cyclotron wave was cut off.

The ELMO machine was operated with up to 1-kW continuous wave of 35.7-GHz power and the magnetic field adjusted for fundamental resonance in the mirror throats at this frequency. An energetic plasma with a $\beta \simeq 5\%$ could be produced. The 10.6-GHz power was operated either pulsed or continuous wave.

B. DIAMAGNETIC ENERGY LOSS MEASUREMENTS

Upon the application of the subresonant 10.6-GHz power, the plasma diamagnetic signal was observed to drop dramatically, indicating plasma energy loss. Figure 13 shows the decrease of perpendicular stored energy vs applied 10.6-GHz LOR power. It is apparent that the stored energy drops approximately linearly with power until all but a small fraction of the stored energy is removed.

A waveguide port in the opposite end of the cavity showed a power transmission rise time approximately equal to the plasma energy decay time, indicating that the power is transmitted only as the energetic plasma is driven out. In addition, the reflected power shows an initial maximum which drops to a minimum near the time when the diamagnetic signal has dropped to its minimum.

Large bursts of x rays were observed with the application of the LOR power. Both radial and axial losses were observed, the radial losses

to radial probes inserted on the midplane and the axial losses to the end walls. A burst of neutrons was also observed. These neutrons were found to be due in part to the deuterium gas and in part to (γ,n) processes on copper requiring ~10-MeV photons. These effects will be discussed later.

Because of the nonsymmetrical arrangement of power introduction, one possible reason for the loss might have been radiation pressure from the end-feed microwave power. Subsequent experiments with balanced feed from both ends showed agreement between energy-loss measurements within a few percent, thus ruling out asymmetric radiation pressure.

The background cold plasma, as indicated by visible light intensity and probe current, showed no observable disturbance as a result of this loss process. The low-level diamagnetic signal remaining probably represented this cold plasma.

The decay time of the perpendicular diamagnetic signal is shown in Fig. 14. At low values of 10.6-GHz power, the decay time is approximately constant and equal to the decay time of the stored energy with 35.7-GHz power turnoff (i.e., no 10.6-GHz power). At high 10.6-GHz power, the decay time goes inversely as the 10.6-GHz power.

Empirical relationships could be derived by assuming that the diamagnetic signal changes were exponential in time, a reasonably good assumption. For the low-power case, that is, $P_{LOR}/P_R < \frac{1}{3}$, where P_{LOR} and P_R are the 10.6-GHz and 35.7-GHz power, respectively, we have found (as mentioned above) that the decay time $\tau \cong$ constant $= \frac{1}{k_2}$ and that the stored energy, $W_\perp$, obeyed the relation,

$$W_\perp(t) \approx \frac{k_1}{k_2} P_R - \frac{k_3 P_{LOR}}{k_2}\left(1 - e^{-k_2 t}\right) , \qquad (1)$$

where k_1 and k_3 are constants of proportionality. Hence the differential equation for the process is

$$\frac{dW_\perp}{dt} \cong k_1 P_R - k_3 P_{LOR} - k_2 W_\perp \quad . \tag{2}$$

We interpret the first term as a linear heating term due to the resonant power, the second term as a linear loss term due to the LOR power, and the third term due to the normal collisional losses of the plasma electrons out the mirror. In the absence of the second term (that is, $P_{LOR} = 0$), we would have an equation for the normal buildup and decay of the resonantly fed plasma. Hence the LOR power represents an additional collisional-like loss process in its effect.

In the long time limit the relationship describing the coefficient of perpendicular velocity space diffusion [18], $B_\perp$, is,

$$< v_\perp^2 > = 4B_\perp t \quad ,$$

where $v_\perp$ is the perpendicular electron velocity. Differentiating by t and assuming $B_\perp$ is not a function of t, we have

$$4B_\perp = \frac{d}{dt} < v_\perp^2 > = \gamma \frac{2}{m_e} \frac{d < E_\perp >}{dt} \quad ,$$

or

$$2\gamma m_e B_\perp = \frac{t}{dt} < E_\perp > \quad ,$$

where m_e is the electron mass, γ is the ratio of the total electron energy to the rest energy, and $E_\perp$ is the perpendicular energy. Hence the rate of change of perpendicular energy is proportional to the coefficient of velocity space diffusion.

Assuming constant 35.7-GHz power, we have from Eq. (2),

$$\left.\frac{dW_\perp}{dt}\right]_{3\text{-cm effect}} = -\,k_3\,P_{LOR} = 2\gamma m_e\,B_\perp\,n_e V \quad .$$

Thus, we have found a direct measurement of $B_\perp$.

Assuming that other loss processes can be neglected, we can calculate the coefficient of perpendicular velocity diffusion as,

$$B_\perp \cong 2 \times 10^{20}\ \mathrm{cm}^2/\mathrm{sec}^3 \quad .$$

Evidence is presented in Sec. 3, D, that the perpendicular spatial diffusion is not appreciably affected by the microwave power, so that the assumption that the process is governed by $B_\perp$ may be good.

For higher power, that is, $P_{LOR}/P_R \gtrsim \frac{1}{3}$, we observed that the decay time $\tau \cong \frac{1}{k_4\,P_{LOR}}$, where k_4 is a constant of proportionality. The perpendicular stored energy followed roughly the equation

$$W_\perp(t) \cong \frac{k_1}{k_2}\,P_R\,e^{-k_4 P_{LOR} t} + W_{\perp o} \quad , \tag{3}$$

where $W_{\perp o}$ was the small residual stored energy remaining as long as the resonant power was left on. The differential equation for this process is then

$$\frac{dW_\perp}{dt} \cong -\,k_4\,P_{LOR}\,W_\perp \quad . \tag{4}$$

Here we have a nonlinear process involving the product of the LOR power and the stored energy. However, this would appear to be a different nonlinear process than that seen in the low-power case.

C. WALL X-RAY ENERGIES

Several more experiments were done on the driven losses. In one set, the "characteristic" energy of the particles striking radial and axial obstructions was measured as a function of the 3-cm power level. These characteristic energies were measured by an absorber transmission technique, because the burst of x rays was too intense to be handled by a pulse-height analyzer. Figure 15 shows the result. Again for low power, $P_{LOR}/P_R \lesssim \frac{1}{3}$, the characteristic energy of the lost particles was the same radially and axially and has the same characteristic energy as the temperature determined from the free-free bremsstrahlung, $\sim$700 to 800 keV. However, at higher LOR power, $P_{LOR}/P_R \gtrsim \frac{1}{3}$, the characteristic energy of the axially lost particles increased. Because of the non-reproducibility of the measurements, it could not be precisely measured, but it clearly rose to a value 1.5 to 2 times larger than the low-power value. The radial characteristic energy did not change an observable amount at high 3-cm power levels.

As shown in Fig. 16, there were differences in the time dependence of the wall x-ray radiation burst produced by the LOR power. The axial loss showed a slow buildup after the application of LOR power, whereas the radial loss showed a prompt loss immediately on application of the power. Occasionally, the radial loss burst would have two or more peaks. However, energy analysis showed no energy change for any of these peaks. It would appear, then, that the LOR power was affecting the energy of the axially lost particles at high LOR power levels, but not that of the radially lost particles. This could either be a heating process, a selection process, or both: for example, particles were either actually

absorbing energy from the LOR power and/or particles in a certain energy range above the plasma temperature would find their diffusion rate into the loss cone suddenly increased.

D. SPATIAL DIFFUSION

A probe was built that could be inserted radially and then be rapidly extracted a distance of ~1 cm in ~10 msec. The x-ray signal from this probe was measured by a collimated NaI crystal and phototube detector. The probe could be moved some milliseconds before the LOR microwave power was pulsed on. The time of the x-ray signal peak was measured while the probe was first held stationary during the microwave pulse and then moved just prior to the microwave pulse. The delay in occurrence of this peak after the probe was withdrawn indicated the radial diffusion velocity of the plasma electrons to the probe. Figure 17 shows the time dependence of the x-ray signals. The average measured values of the diffusion velocity were from 4 to 8 cm/sec. When the probe was moved but the microwave power not pulsed, the x-ray signal dropped and then rose exponentially to a new equilibrium level, as shown at the bottom of the figure. The e-folding time for this rise associated with the ~1-cm probe motion indicated a normal radial diffusion velocity of ~4 cm/sec. We would conclude from this that the radial diffusion velocity might be increased by as much as a factor of 2 by the LOR microwave power, but was not increased by an order of magnitude. In the long time limit, the spatial perpendicular diffusion coefficient [20] is given by $< r^2 > = 4D_\perp t$. Taking t as the e-folding time and $\sqrt{< r^2 >}$ as the distance the probe moved, we find $D_\perp \cong 1$ cm^2/sec for the nondriven perpendicular motion and $D_\perp \cong 2$ cm^2/sec for the driven loss. Since the value of $D_\perp$ is not affected strongly by the LOR power, our assumption of $B_\perp$ being the dominant process may be reasonable.

E. NEUTRONS

The neutron burst resulting from the LOR power pulses was analyzed by a pulse-height analyzer in the time mode (i.e., operated as a multiscaler). In order to accumulate a sufficiently high count for good statistics, a large number of pulses (~100) were used to trigger the time mode. The neutrons were counted in 10-msec channel intervals. Figure 18 shows one of the counts made by operating with D_2 gas and then subsequently operating with H_2 gas after a long baking process to remove the wall-embedded D_2. The D_2-H_2 difference curve should accurately represent the D_2 gas effect alone since all other parameters have been held constant.

With the D_2 gas, a prompt buildup of the neutron count is observed with a buildup time of ~80 msec. With H_2 gas, this prompt buildup is missing but a later peak occurs after an apparent delay of ~80 msec and a buildup time of ~50 msec. A series of runs has shown that these buildup and delay times are all roughly proportional to P_{LOR}^{-1}, in qualitative agreement with most heating theories. However, because of the difficulty in averaging over the electron energy distribution and the neutron production cross sections, no quantitative agreement can be calculated.

The neutrons with H_2 gas can only be accounted for by wall processes, and the most reasonable explanation is (γ,n) processes on copper. These require photon energies of $\gtrsim$ 10 MeV and imply either a selective loss of particles above this energy by the LOR radiation or a heating of particles to these energies by the LOR radiation. The long delay is indicative of a long heating time needed for electrons to gain many MeV. It would appear that some heating is occurring, since the buildup of the neutron count rate

in the D_2-H_2 difference curve can best be accounted for by an increase in electrons with energy over 2.22 MeV rather than an increase in cold plasma ions. As mentioned earlier, cold plasma current to probes does not change during a LOR pulse. Also, there is a tail on the neutron pulse after the LOR power pulse ends, implying that some electrons have been heated and are relaxing back to an equilibrium. The decay time of this tail is ~100 msec, which is too long to be accounted for by a gas equilibrium time alone. The sharp discontinuity in the count rate at the end of the microwave pulse is not understood.

The H_2 gas neutron count rate is reduced by a factor of ~3 when a radial probe is inserted by about one inch. If there is an acceleration process occurring, this would mean that it is near the wall and it is disturbed by a radially inserted obstruction. Copper probes show an approximately 10-min positron half-life after operation, indicating that some energetic (>10 MeV) electrons are striking the probe and producing ^{62}Cu activity. This activity is not seen in the absence of LOR power. When operating with D_2 gas, ^{10}B-coated probes show no 20-min activity. A positive indication would imply (d,n) processes with deuteron energies of tens to hundreds of keV [21]. Hence there is no evidence for the creation of a large space charge or resonant rf fields by this process.

F. CALORIMETRIC MEASUREMENTS

Calorimetric probes were constructed to measure the energy content of the plasma striking them. One probe was inserted radially into the cavity. The probe was equipped with a copper tip of sufficient radial extent to intercept almost all of the large orbit particles lost radially during a burst. The sensitive element was a thermistor whose resistance

change indicated the temperature rise of the copper tip and hence the energy input. A long time constant thermal leak to the demineralized water system provided an equilibrium temperature. The probe was calibrated with a resistor thermally connected to the front surface. A correction was made for both the increased thermal capacity of the resistor and for the long thermal transmission time from the resistor to the thermistor.

For a given input of LOR power (pulsed in 1-sec bursts for convenience), Fig. 19 shows that the total amount of energy deposited on the probe amounted to ~10% of the stored energy measured diamagnetically. There was no apparent absorption of the LOR energy by those plasma electrons which struck the radial probe. Although up to 3 kJ of LOR energy was injected, only a fraction of the plasma energy already present was deposited on the probe.

Normal (nondriven) flutelike instabilities were also measured with this probe. As shown in Fig. 19, about half of the energy lost by the instability (as measured by the diamagnetic drop) appeared on the radial probe. This energy loss was always higher than that obtained by the LOR power pulse in the absence of instabilities.

Figure 20 shows the amount of energy deposited on the probe as a function of LOR power. It is clear that there is a saturation value independent of the input LOR energy. The amount of energy appears to increase monotonically with LOR power up to a value near this saturation value.

Corresponding measurements made on the axial losses show some LOR energy absorption by the axially lost particles. The axial calorimeter,

previously mentioned in Sec. 2, B, 3, was used to measure the plasma energy ejected through the mirror throat by a pulse of LOR power above the equilibrium power input generated by the plasma flow out the mirror.

Figure 21 shows a calorimeter scan at the mirror throat similar to that shown in Fig. 9. The energy clearly comes out of the annular region previously determined from skimmer probe and magnetic probe measurements. The mean radius in the figure is ~9 cm on the upper abscissa scale. This measurement must again be corrected for the increased area with probe radius placing the peak at ~11 cm, still in qualitative agreement with the other measurements.

With low values of LOR power (that is, 50 W in the figure) only a fraction of the energy is removed from the machine. At the 200-W LOR power level, diamagnetic measurements show almost all the energy is removed and at this input power level the calorimeter energy level saturates at the position of the annulus. At higher values of LOR power (that is, 1000 W in the figure), no more energy comes out of the annulus at the peak position but the annulus is clearly broadened. It appears that the broadening is due both to the radial diffusion previously described and to some heating of the plasma electrons during the LOR power pulse.

The amount of heating could not be determined for the reason previously mentioned; the energy flow was not azimuthally symmetric. Hence a power and energy balance could not be accurately made. However, calculations showed that more energy was coming out of the plasma than had been stored in the energetic electrons.

4. SUMMARY

Off-resonant heating of electrons by microwaves is found to be an effective method if the frequency is above the cold-electron gyrofrequency. The enhanced efficiency is believed to be due to two probable effects, stochastic heating and control of an instability through reduction of the anisotropy of the distribution function or relativistic effects. When power is applied to the plasma at frequencies below the cold-electron gyrofrequency, the plasma is expelled from the mirror, although a few electrons are heated.

ACKNOWLEDGEMENTS

The authors wish to acknowledge the assistance of the technical staff: R. L. Livesey, M. W. McGuffin, M. Maskewitz, and G. Bryson. Some of the supporting experiments were aided by S. T. Nolan and W. B. Ard. We are indebted to N. H. Lazar, W. B. Ard, F. R. Scott, and J. C. Sprott for interesting and valuable discussions. We gratefully acknowledge the interest and support of A. H. Snell and H. Postma.

REFERENCES

[1] BECKER, M. C., DANDL, R. A., EASON, H. O., Jr., ENGLAND, A. C., KERR, R. J., and ARD, W. B., Nucl. Fusion: 1962 Supplement, Pt. 1 (1962) 345.

[2] ARD, W. B., DANDL, R. A., ENGLAND, A. C., HAAS, G. M., and LAZAR, N. H., in Plasma Physics and Controlled Nuclear Fusion Research (Proc. Conf. Culham, 1965) 2, IAEA, Vienna (1966) 153.

[3] ARD, W. B., BECKER, M. C., DANDL, R. A., EASON, H. O., ENGLAND, A. C., and HAAS, G. M., Proc. Colloque Intern. sur l'Intéraction des Champs H.F. Associés a un Champ Magnétique Statique Avec un Plasma (Saclay, France, 1964) 38 (Paris, Presses Univ. de France, 1965; CONSOLI, T., Ed.).

[4] DANDL, R. A., Bull. Am. Phys. Soc. 12 (1967) 461; DANDL, R. A., EASON, H. O., EDMONDS, P. H., and ENGLAND, A. C., in Relativistic Plasmas: The Coral Gables Conf. (BUNEMAN, O., and PARDO, W. B., Eds.) 181 (W. A. Benjamin, Inc., New York, 1968); also, DANDL, R. A., EASON, H. O., EDMONDS, P. H., and ENGLAND, A. C., 2ème Colloque Intern. sur les Interactions entre les Champs Oscillants et les Plasmas (Saclay, France, 1968), Vol. I, 161 (CONSOLI, T., Ed.).

[5] DANDL, R. A., DUNLAP, J. L., EASON, H. O., EDMONDS, P. H., ENGLAND, A. C., HERRMANN, W. J., and LAZAR, N. H., in Plasma Physics and Controlled Nuclear Fusion Research (Proc. Conf. Novosibirsk, 1968) 2, IAEA, Vienna (1969) 435.

[6] DANDL, R. A., ARD, W. B., EASON, H. O., EDMONDS, P. H., ENGLAND, A. C., and NOLAN, S. T., Bull. Am. Phys. Soc. 14 (1969) 1019.

[7] DANDL, R. A., Bull. Am. Phys. Soc. 14 (1969) 1270.

[8] GRAWE, H., Plasma Phys. 11 (1969) 151.

[9] EDMONDS, P. H., DANDL, R. A., and EASON, H. O., Bull. Am. Phys. Soc. 13 (1968) 1490.

[10] IKEGAMI, H., 2ème Colloque Intern. sur les Interactions entre les Champs Oscillants et les Plasmas (Saclay, France, 1968), Vol. I, 429 (CONSOLI, T., Ed.).

[11] DANDL, R. A., EASON, H. O., EDMONDS, P. H., ENGLAND, A. C., and SNELL, A. H., Plasma Phys. 12 (1970) 235.

[12] TIMOFEEV, A. V., Soviet Phys.-JETP 12 (1961) 281.

[13] GUEST, G. E. and SIGMAR, D. J., Nuclear Fusion 11 (1971) 151.

[14] BENFORD, G., BOOK, D. L., CHRISTOFILOS, N. C., FOWLER, T. K., NEIL, V. K., and PEARLSTEIN, L. D., in Plasma Physics and Controlled Nuclear Fusion Research (Proc. Conf. Novosibirsk, 1968) 2, IAEA, Vienna (1969) 981.

[15] BUDKER, G. I., VOLOSOV, V. I., MOISEEV, S. S., PALCHIKOV, V. E., TSEL'NIK, F. A., in Plasma Physics and Controlled Nuclear Fusion Research (Proc. Conf. Culham, 1965) 2, IAEA, Vienna (1966) 245.

[16] SEIDEL, M., Plasma Phys. (J. Nuc. Energy, Part C) 6 (1964) 597.

[17] PILIYA, A. D. and FRENKEL, V. Ya., Sov. Phys.-Tech. Phys. 9 (1965) 1356 and 1364.

[18] ELDRIDGE, O., ORNL-4545 (Thermonuclear Division Annual Progress Report, Dec. 31, 1969) 32 (available from the Clearing House for Federal Scientific and Technical Information); also, Bull. Am. Phys. Soc. 15 (1970) 1407.

[19] SPROTT, J. C., Bull. Am. Phys. Soc. 15 (1970) 1472; also, Physics of Fluids (to be published).

[20] ELDRIDGE, O., private communication.

[21] MARION, J. B., BONNER, T. W., and COOK, C. F., Phys. Rev. 100 (1955) 847.

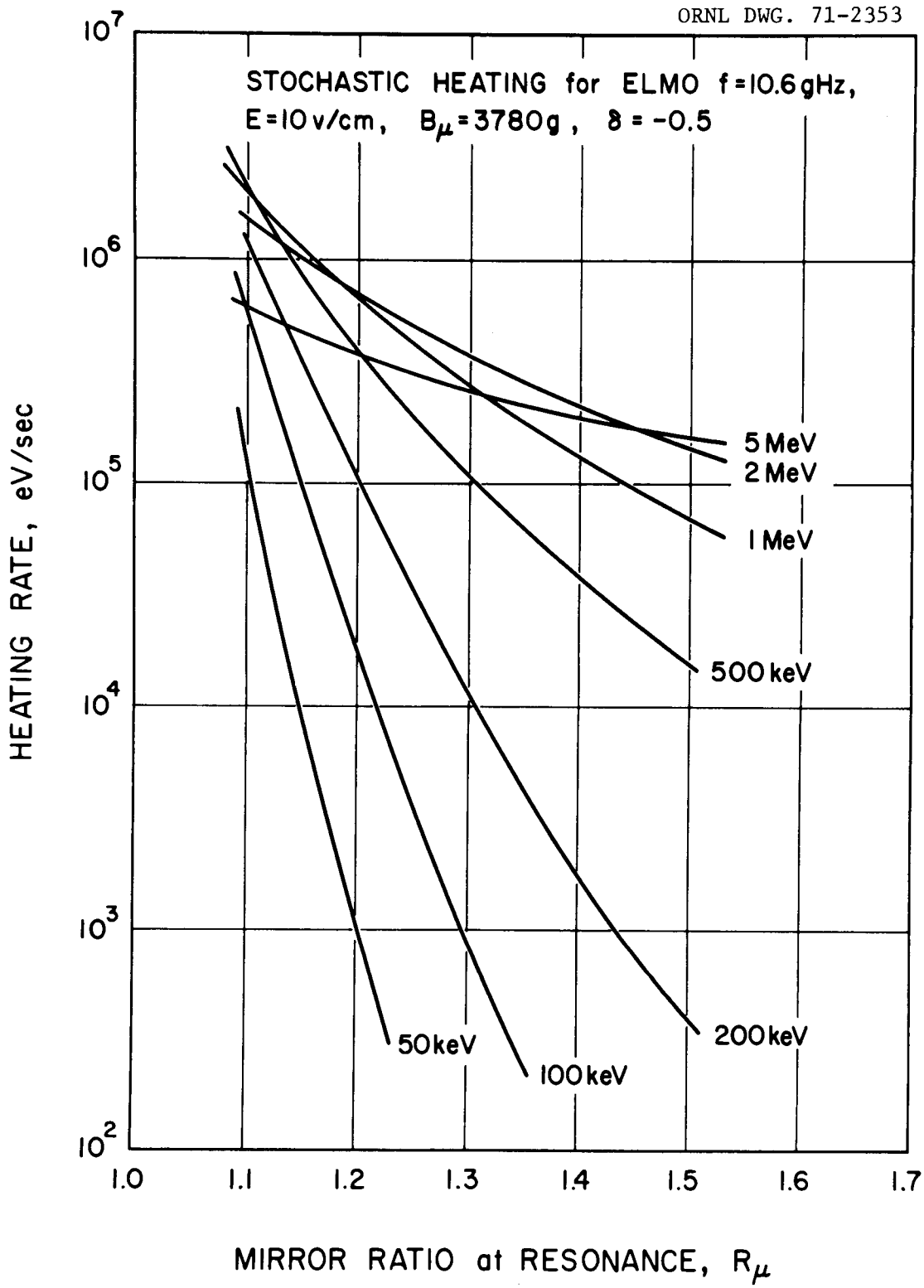

Fig. 1. Heating Rate vs Resonant Mirror Ratio.

ORNL DWG. 70-1091A

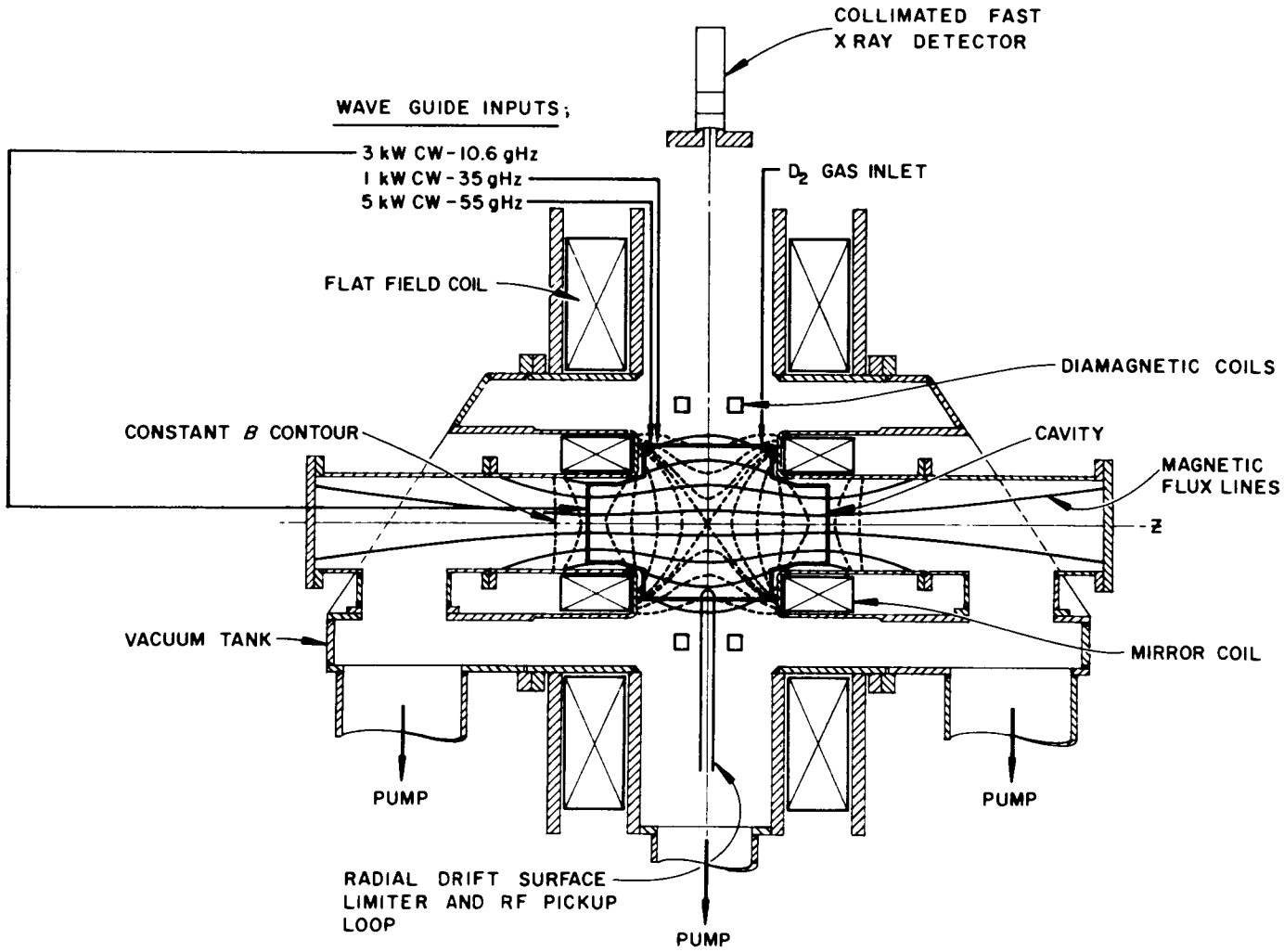

Fig. 2. ELMO Schematic.

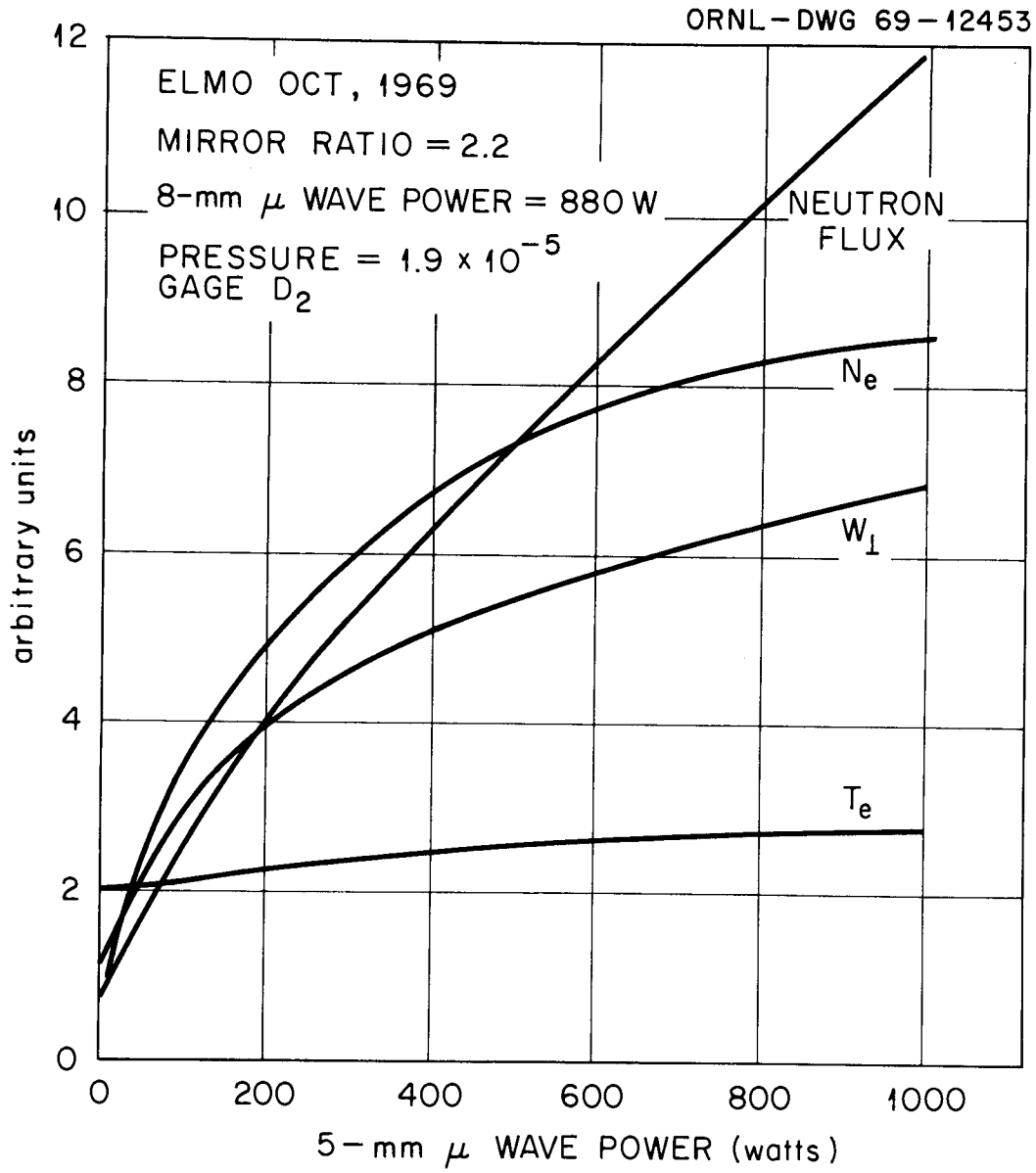

Fig. 3. Heating by Upper Off-Resonant Power at 55 GHz.

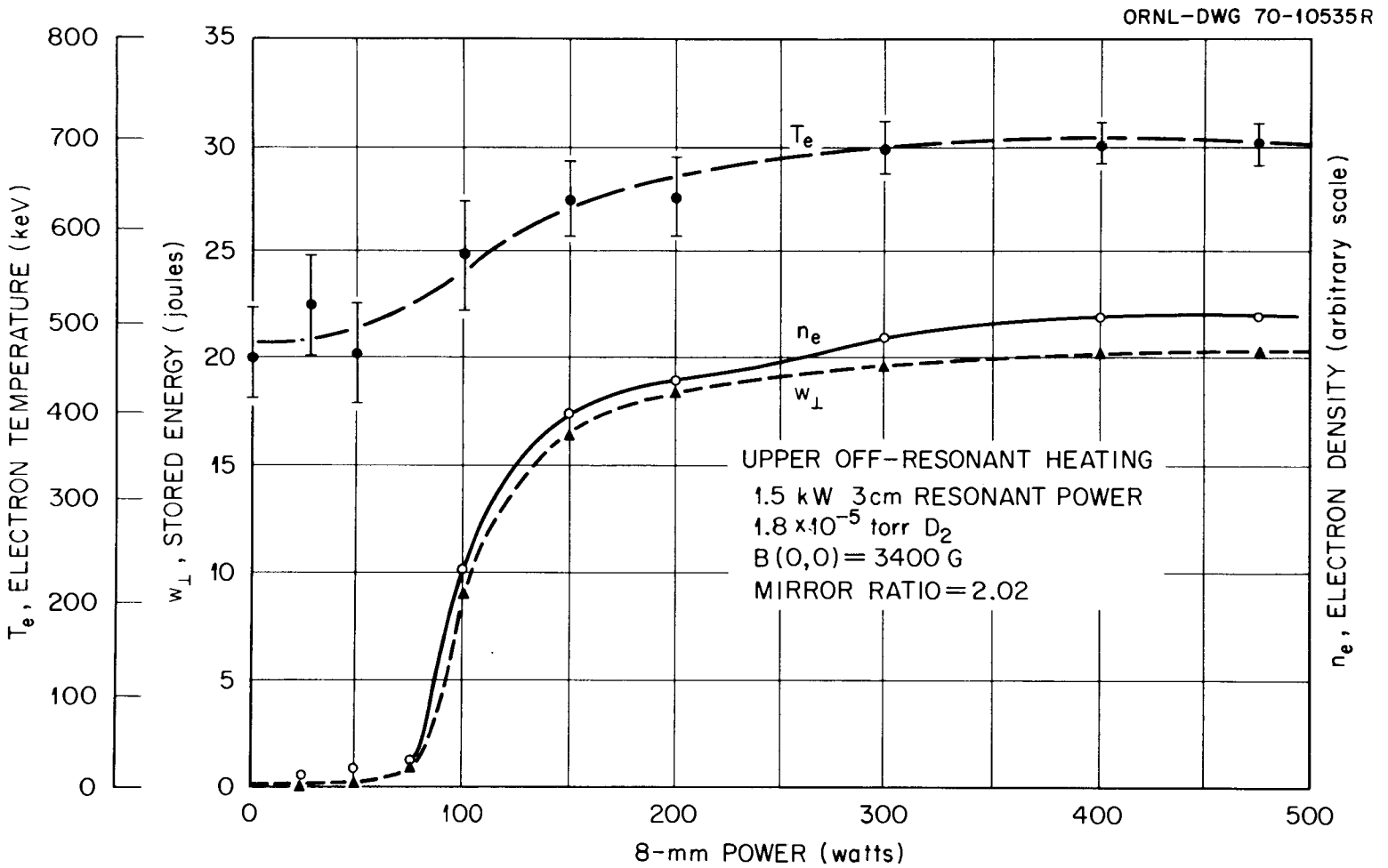

Fig. 4. Heating by Upper Off-Resonant Power at 35.7 GHz.

ORNL-DWG 67-9217AR1

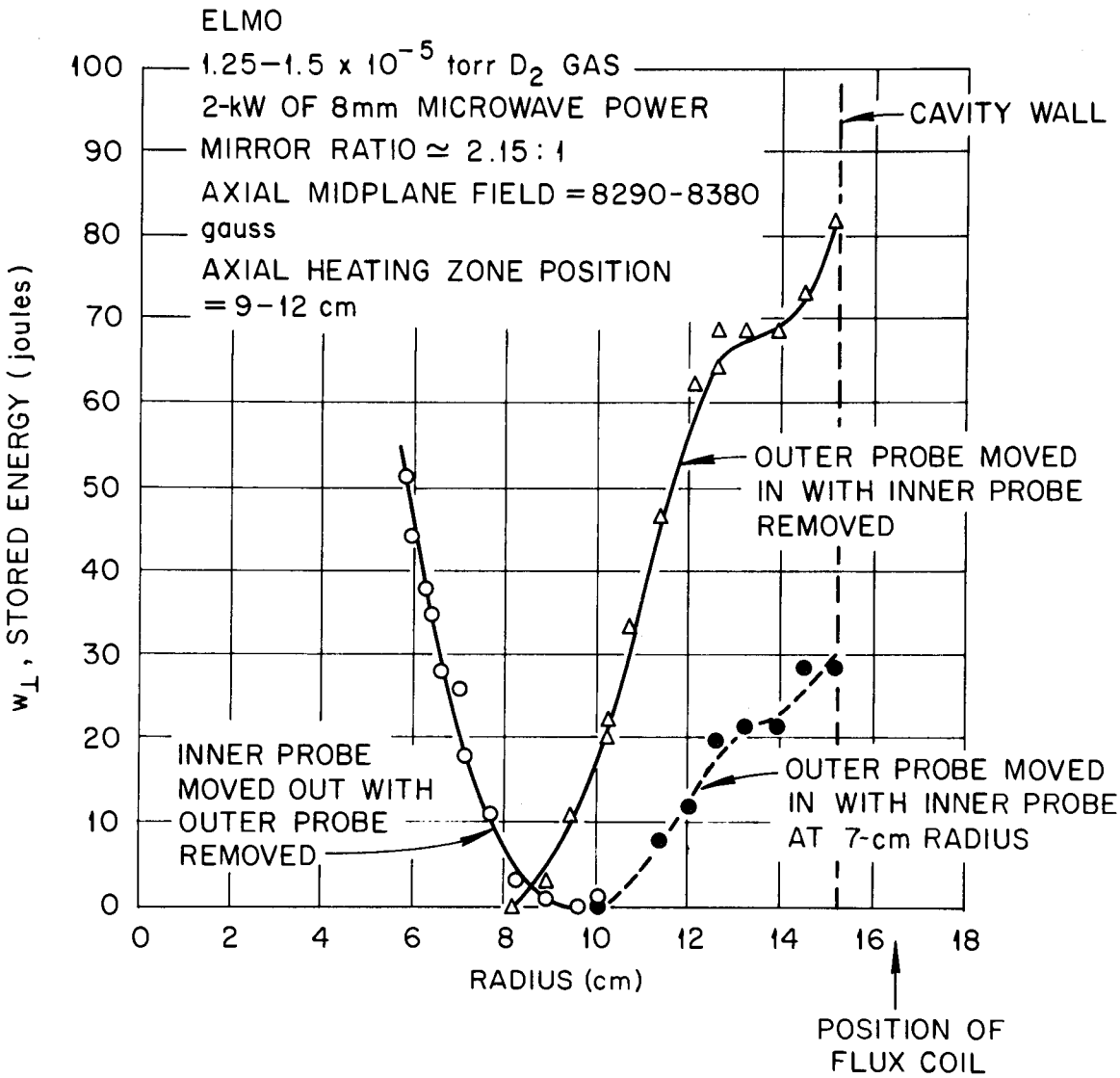

Fig. 5. Skimmer Probe Scans Inside and Outside for Resonant Heating.

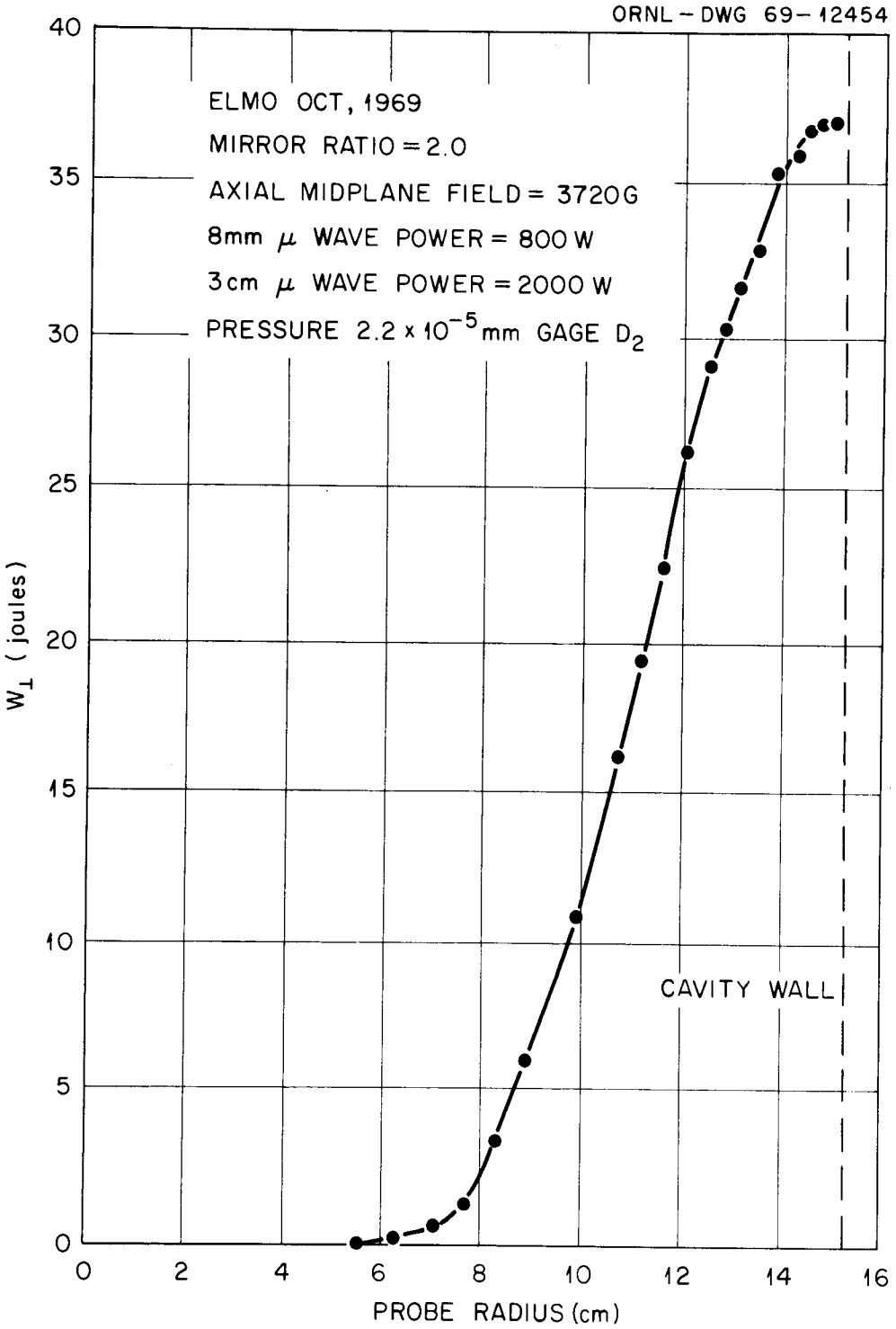

Fig. 6. Skimmer Probe Scan from the Outside Inward for Upper Off-Resonant Heating.

ORNL DWG. 68-13156

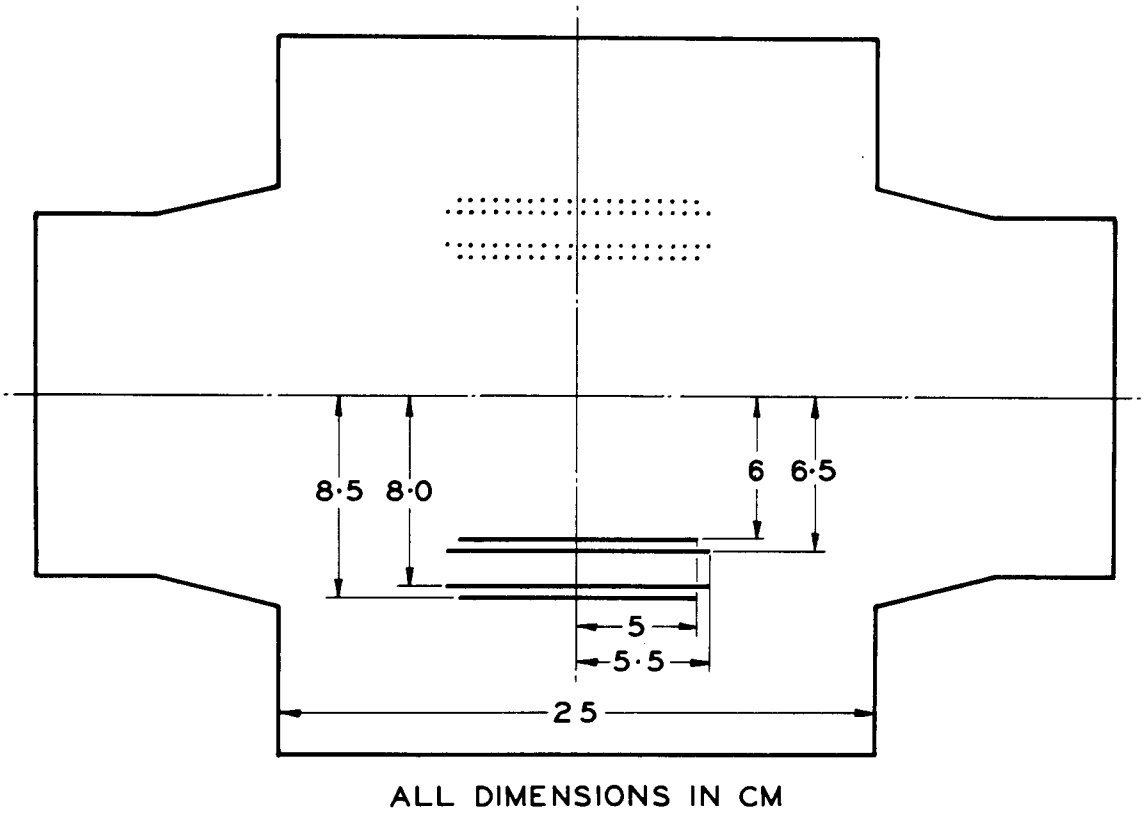

Fig. 7. Current Distribution Calculated from Magnetic Probe.

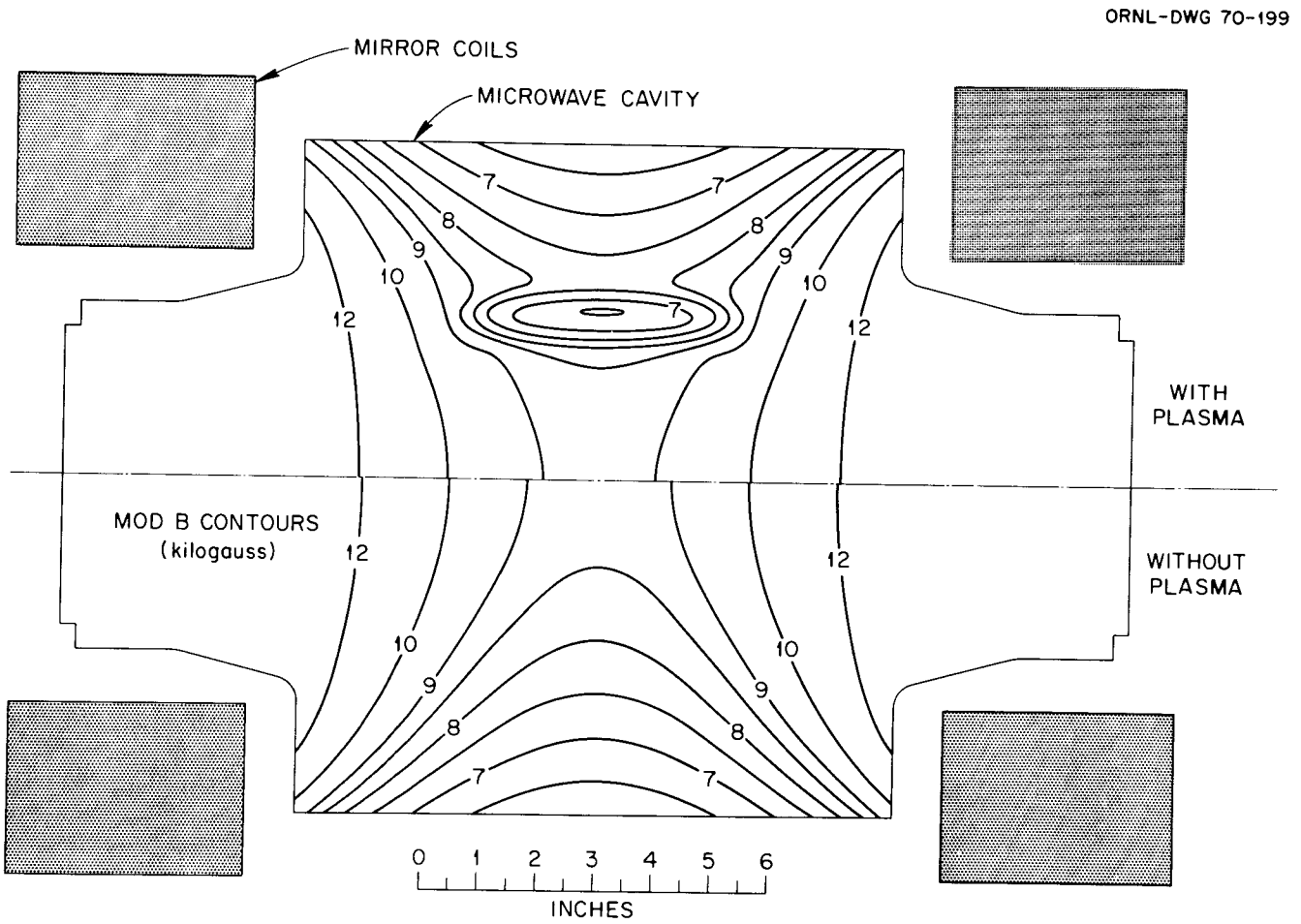

Fig. 8. Mod-B Contours for Self-Consistent Field.

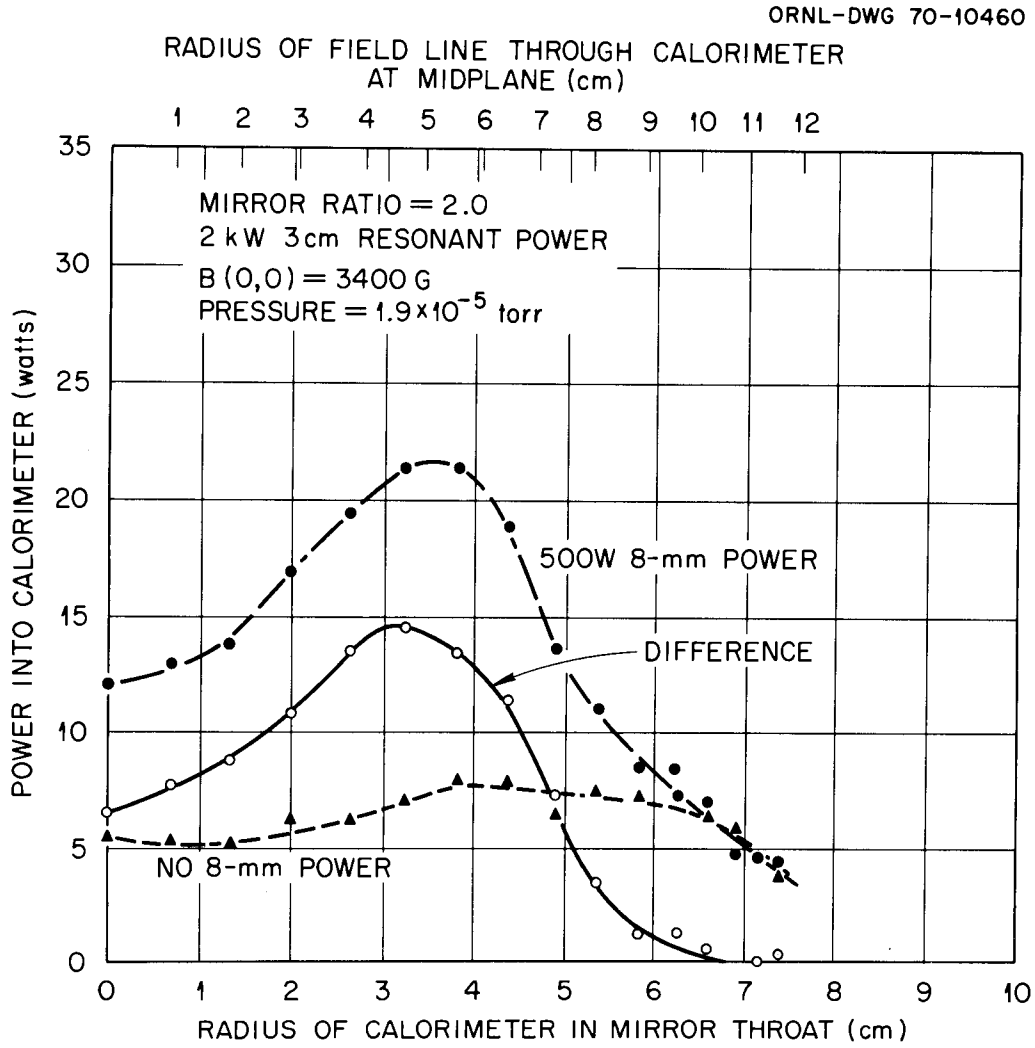

Fig. 9. Power on Calorimeter as a Function of Radius for 10.6 GHz and 35.7 GHz.

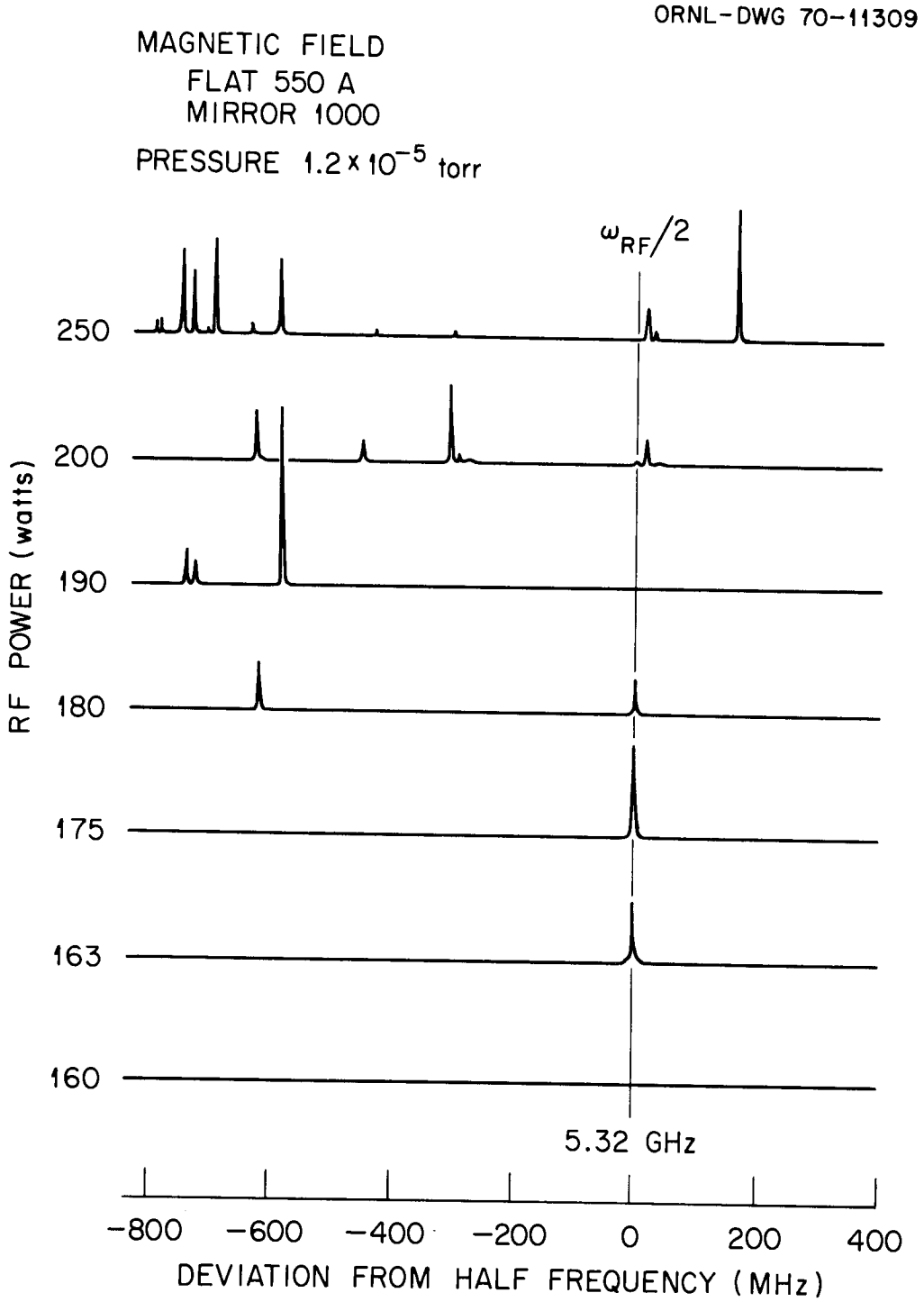

Fig. 10. Spectrum Analyzer Display as a Function of 10.6 GHz Power.

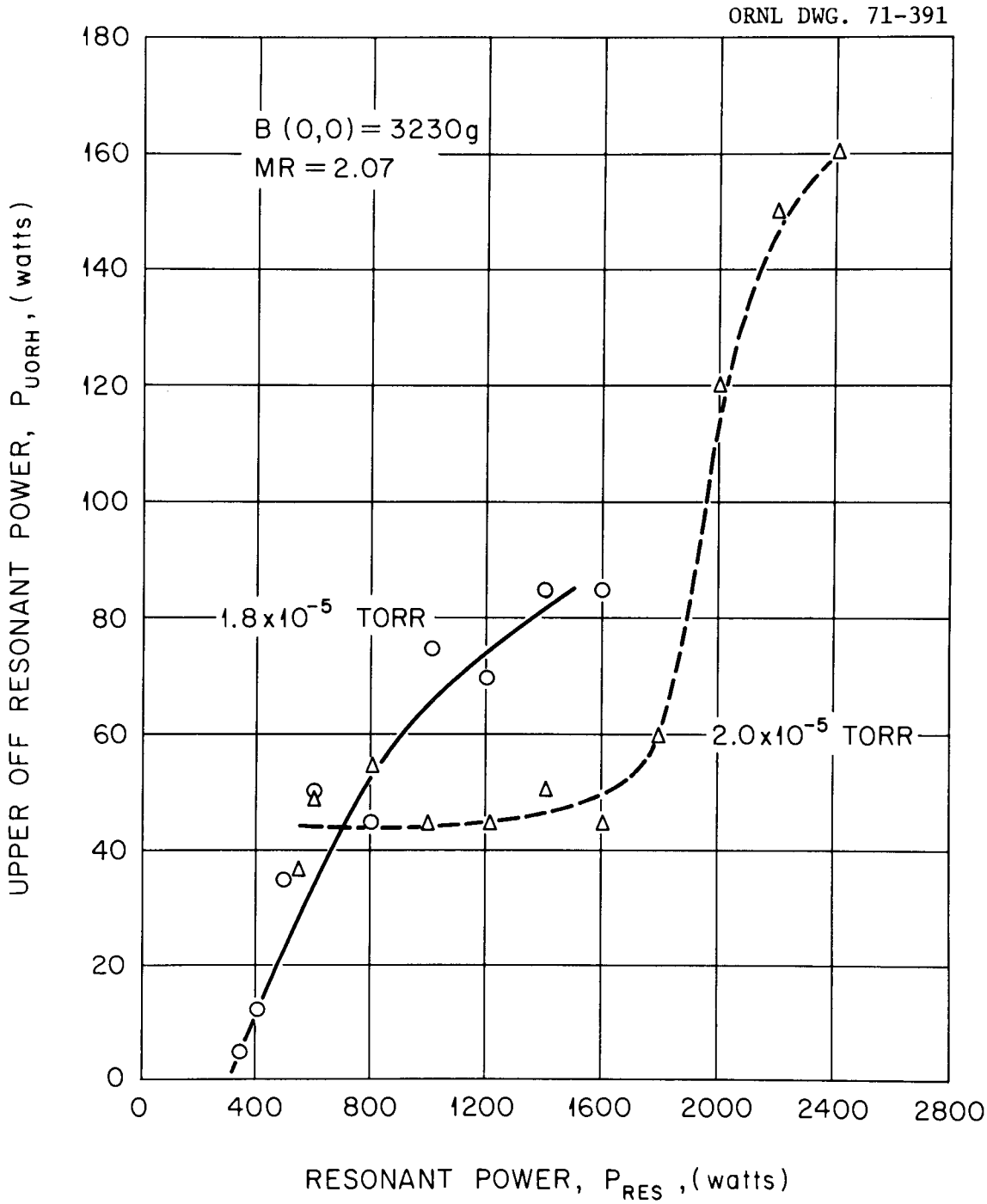

Fig. 11. Upper Off-Resonant Power to Suppress Instability.

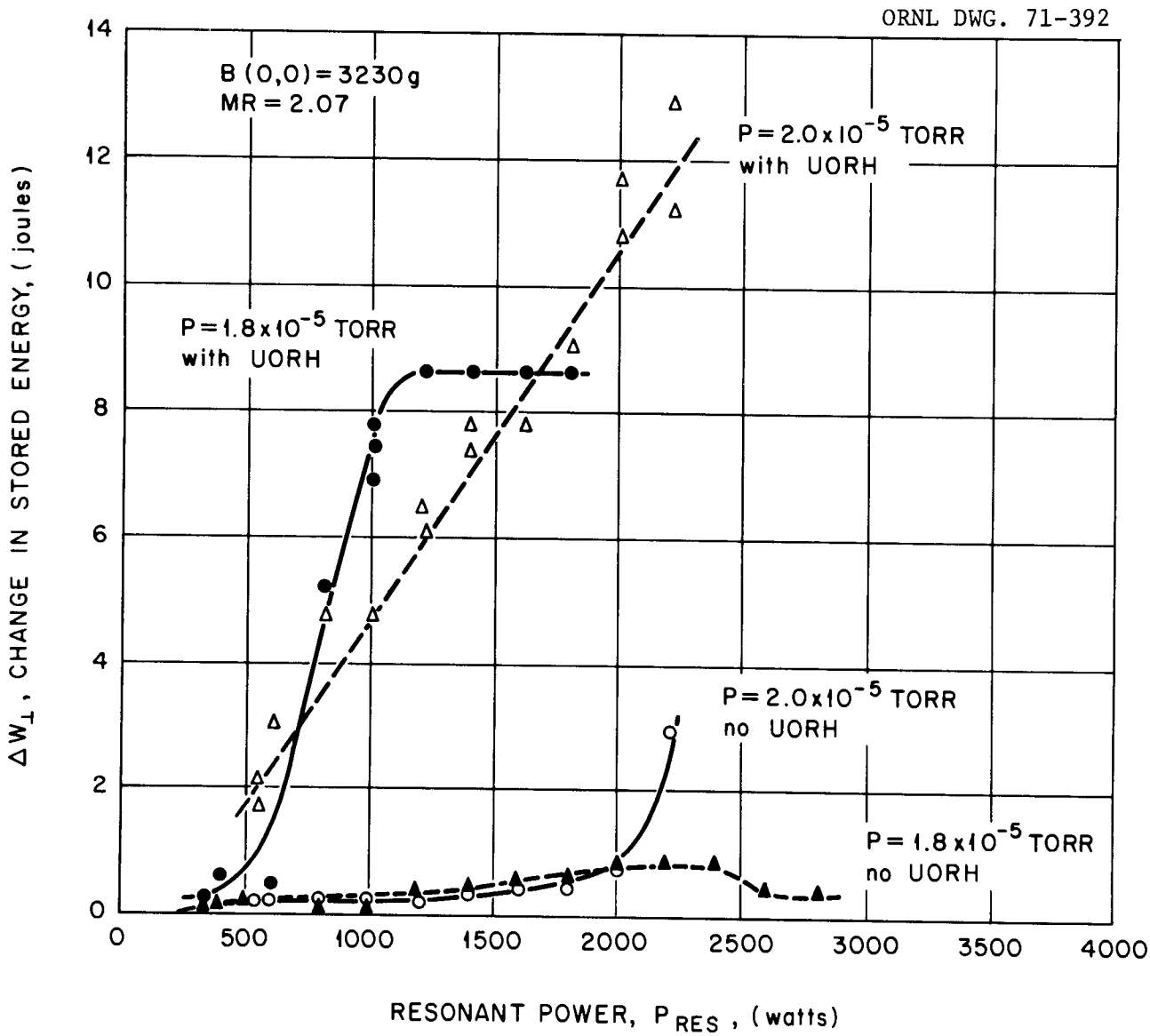

Fig. 12. Stored Energy Produced by Upper Off-Resonant Heating to Suppress Instability.

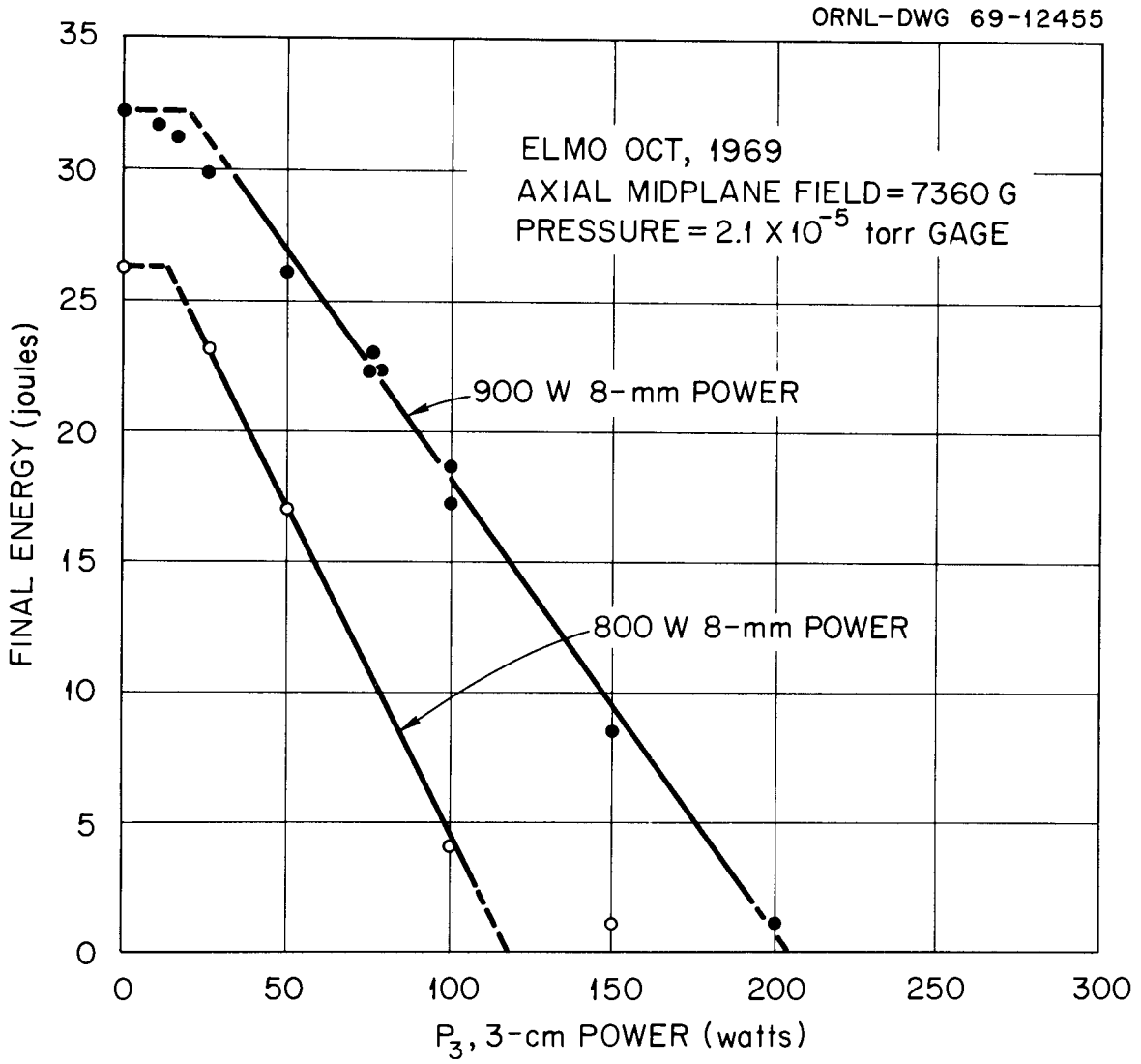

Fig. 13. Stored Energy vs Lower Off-Resonant Power.

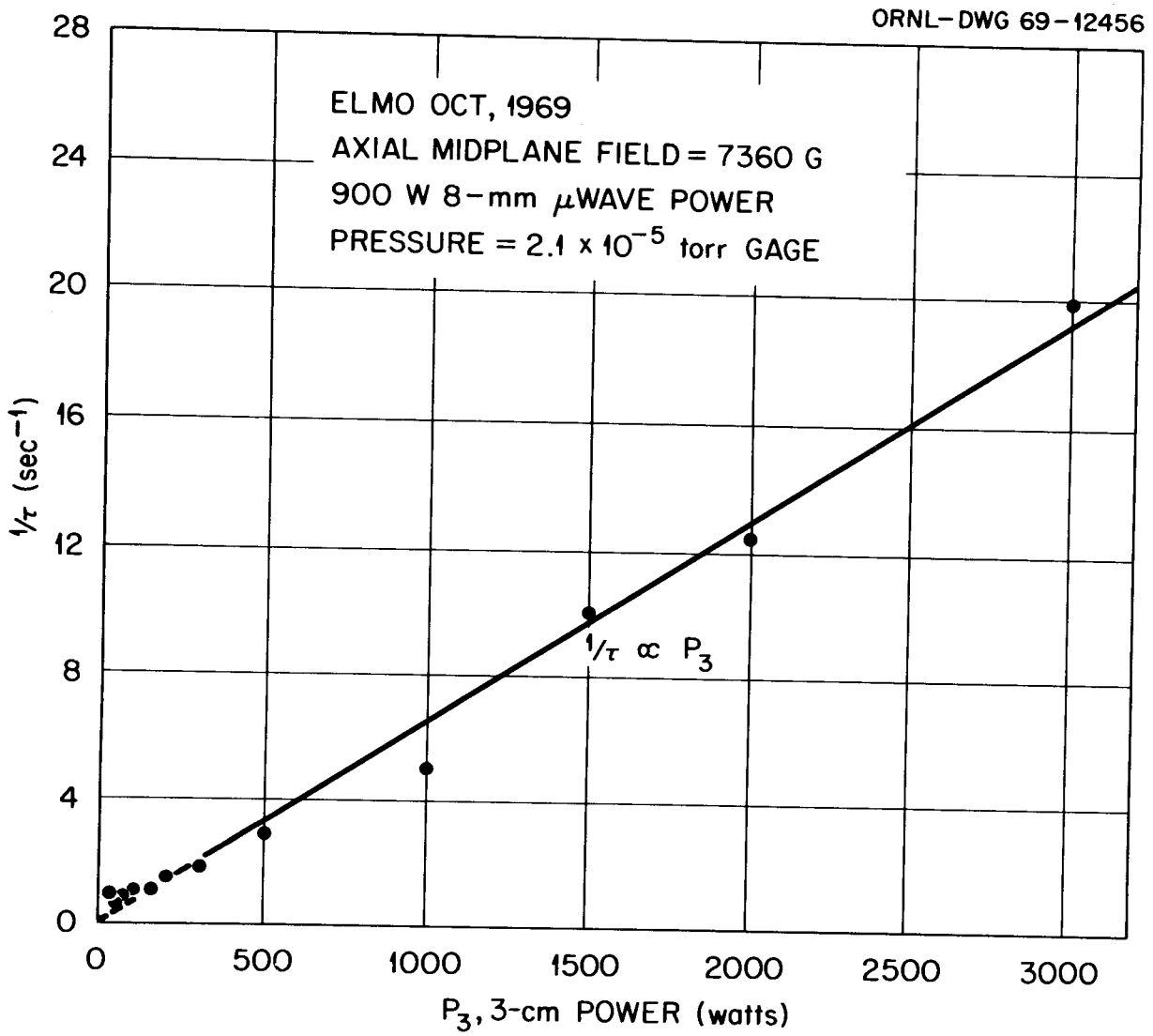

Fig. 14. Decay Time vs Lower Off-Resonant Power.

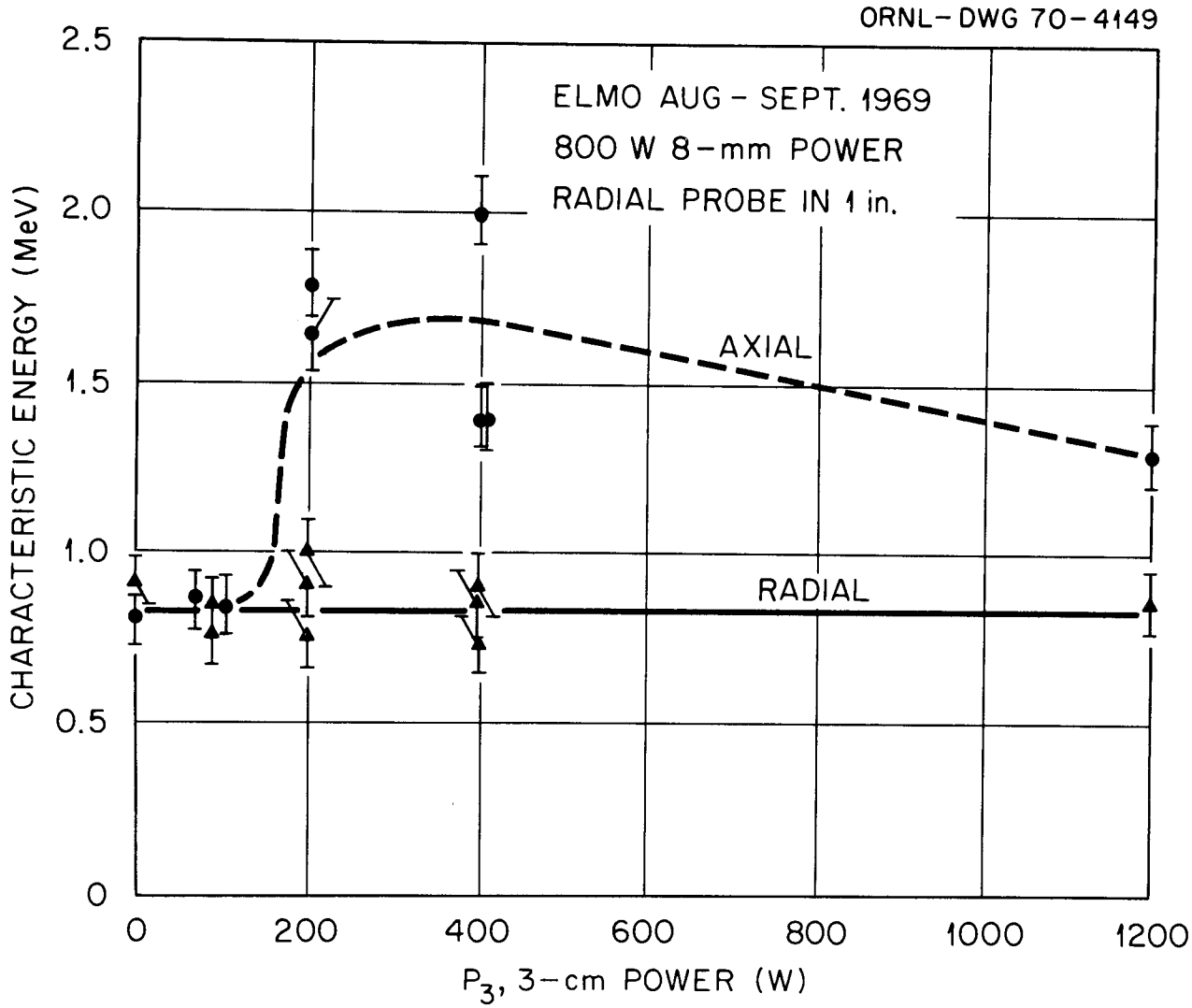

Fig. 15. Wall X-Ray Energies vs Lower Off-Resonant Power.

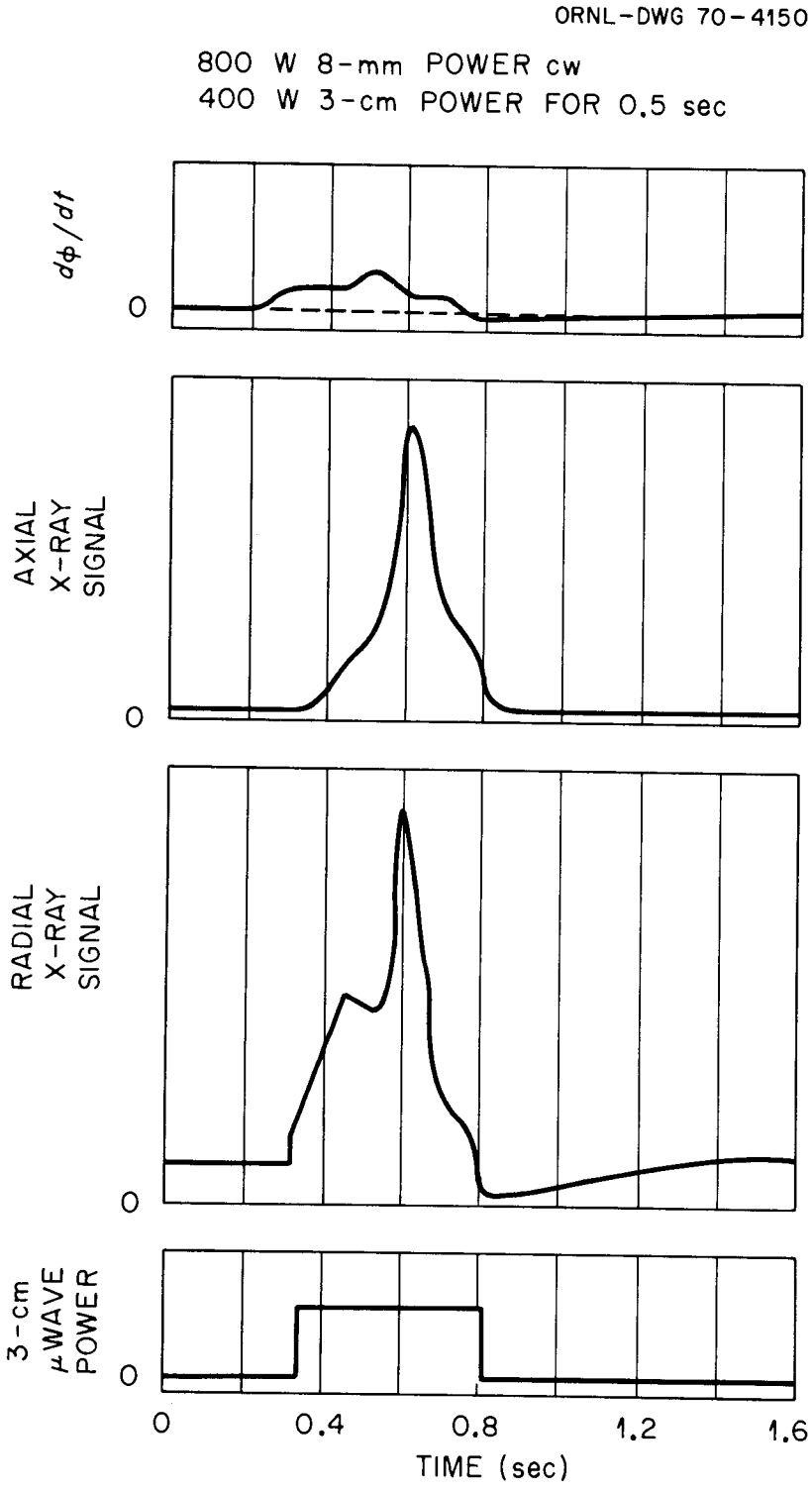

Fig. 16. Wall X-Ray Energy Time Dependence.

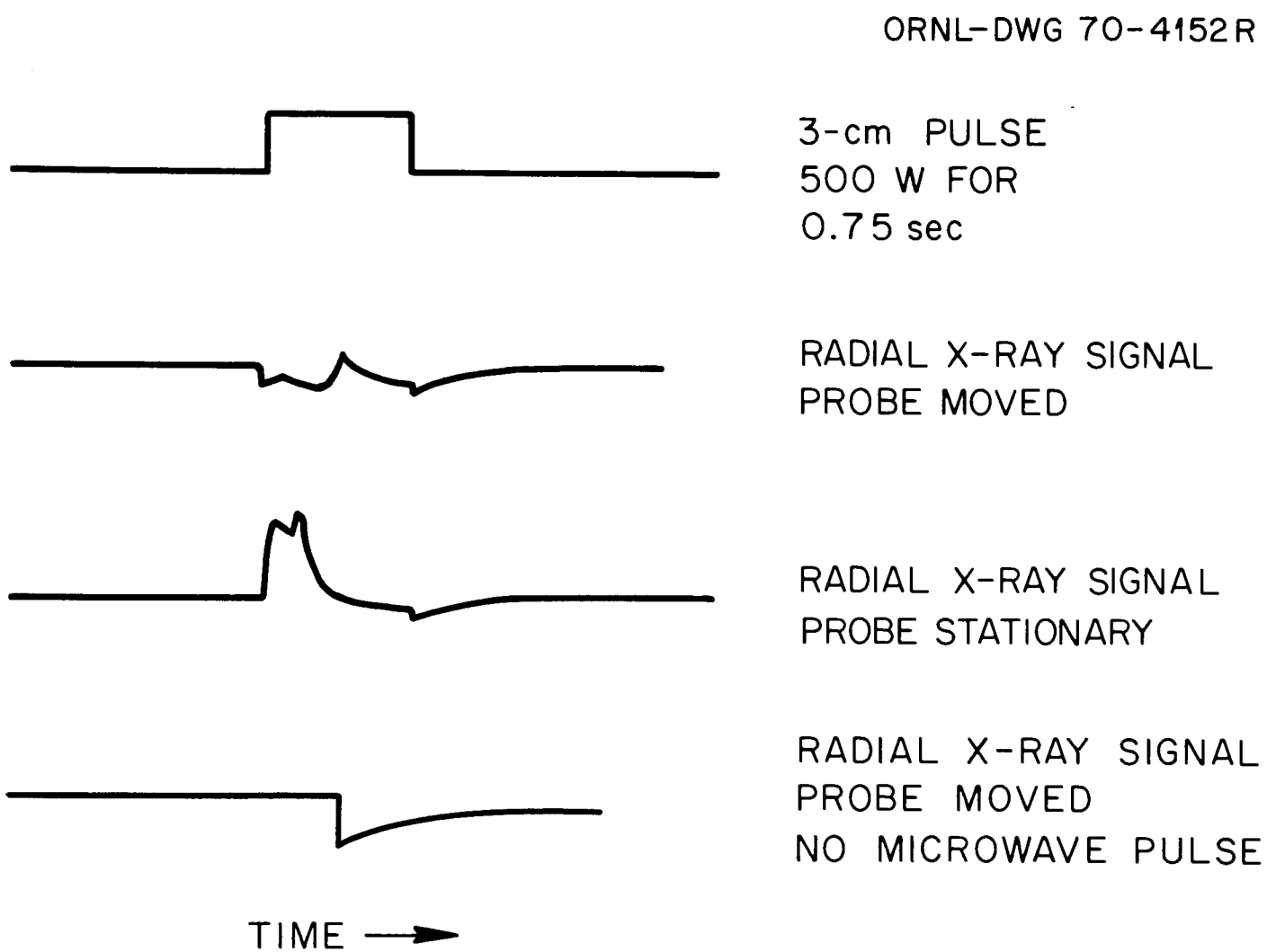

Fig. 17. Time Dependence of X-Ray Signals from Movable Probe.

ORNL DWG. 70-13708

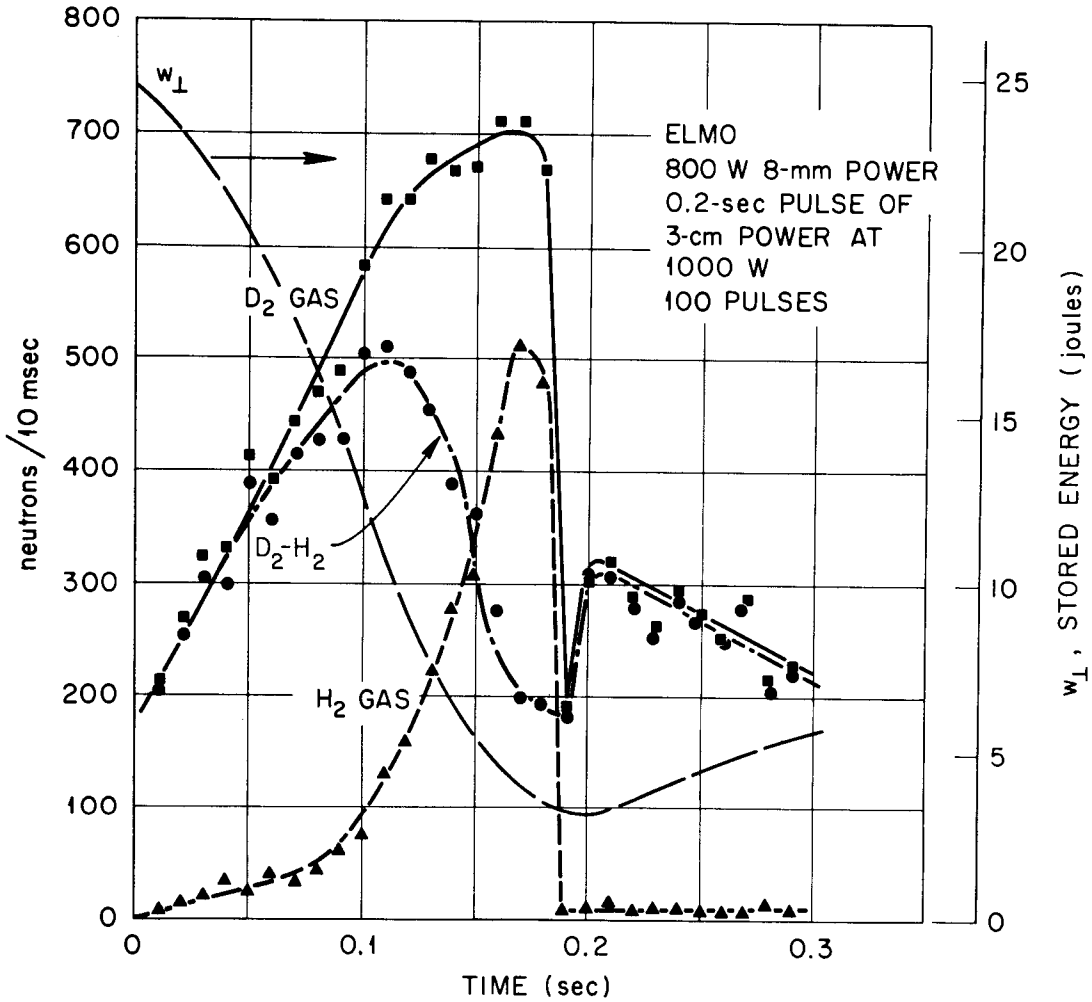

Fig. 18. Neutron Rate Time Dependence with Lower Off-Resonant Power.

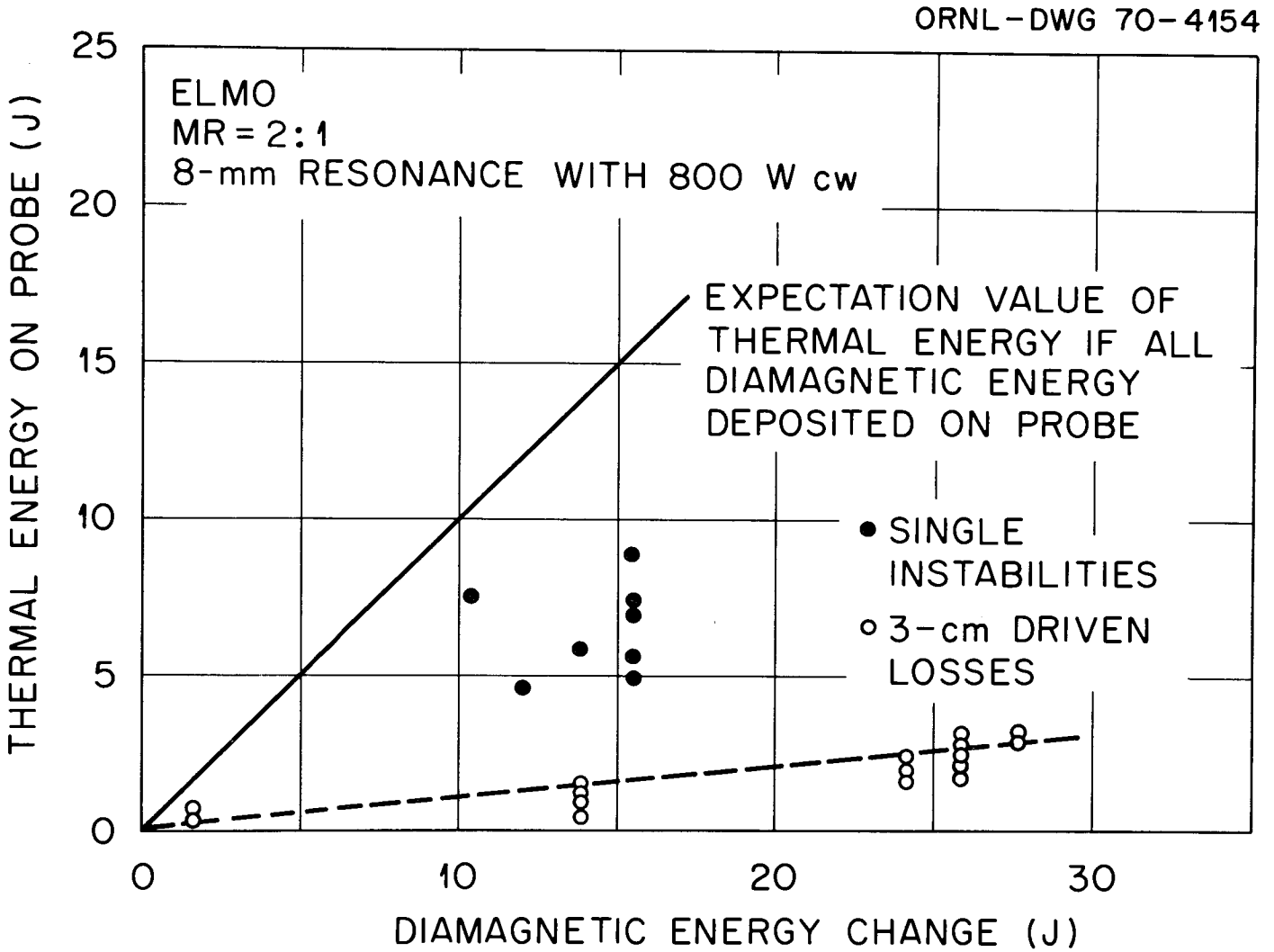

Fig. 19. Energy Deposited on Radial Probe as a Function of Energy Lost.

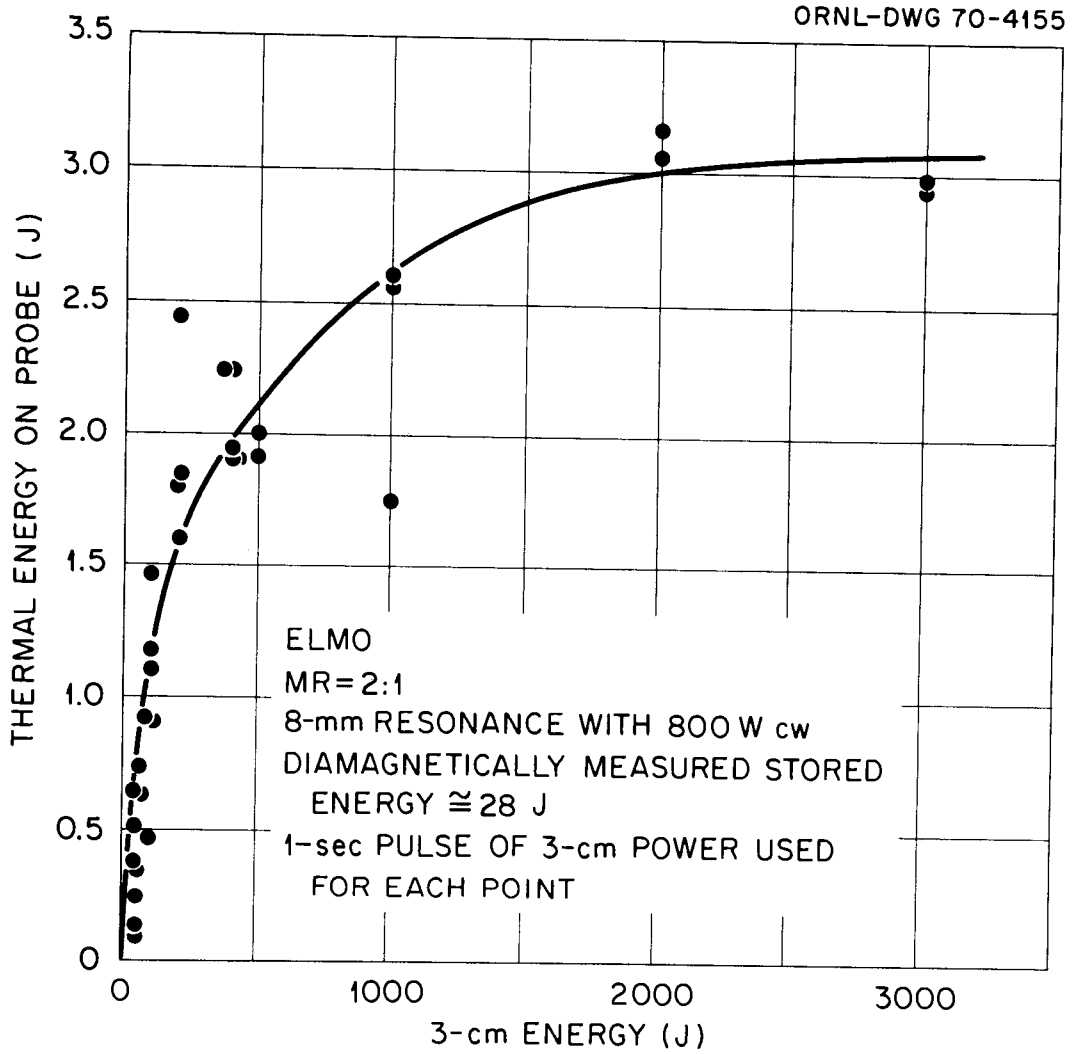

Fig. 20. Energy Deposited on Radial Probe vs Lower Off-Resonant Power.

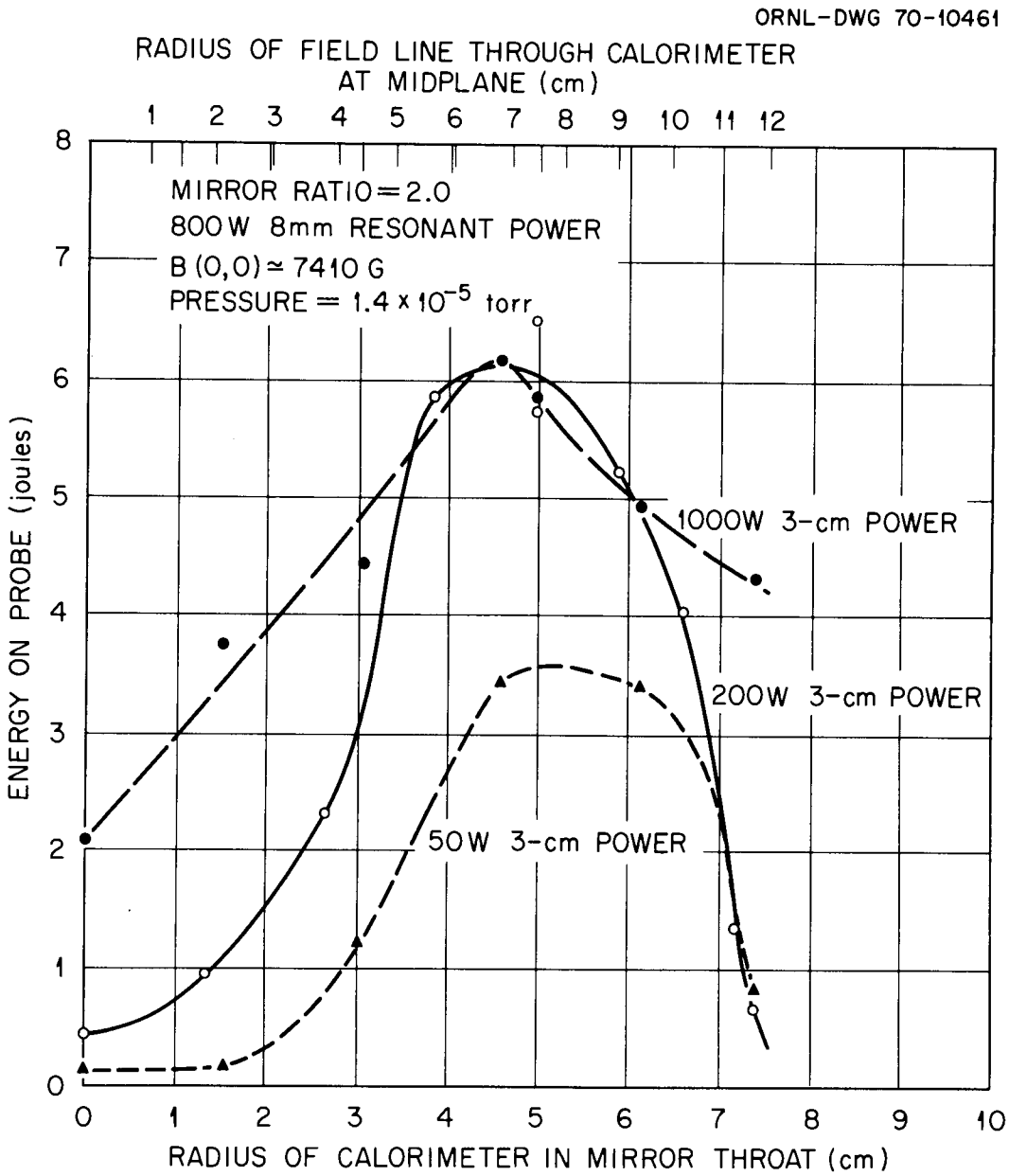

Fig. 21. Calorimeter Scan of Energy Lost Axially with Lower Off-Resonant Power.